

An SDE for Modeling SAM: Theory and Insights

Enea Monzio Compagnoni[†], Antonio Orvieto[‡], Luca Biggio[‡],
 Hans Kersting^{*}, Frank Norbert Proske[§], Aurelien Lucchi[†]

[†] Department of Mathematics & Computer Science, University of Basel, Basel, Switzerland.

[‡] Department of Computer Science, ETH Zürich, Zürich, Switzerland.

^{*} Inria, Ecole Normale Supérieure PSL Research University, Paris, France.

[§] Department of Mathematics, University of Oslo, Oslo, Norway.

Abstract

We study the SAM (Sharpness-Aware Minimization) optimizer which has recently attracted a lot of interest due to its increased performance over more classical variants of stochastic gradient descent. Our main contribution is the derivation of continuous-time models (in the form of SDEs) for SAM and its unnormalized variant USAM, both for the full-batch and mini-batch settings. We demonstrate that these SDEs are rigorous approximations of the real discrete-time algorithms (in a weak sense, scaling linearly with the step size). Using these models, we then offer an explanation of why SAM prefers flat minima over sharp ones – by showing that it minimizes an implicitly regularized loss with a Hessian-dependent noise structure. Finally, we prove that perhaps unexpectedly SAM is attracted to saddle points under some realistic conditions. Our theoretical results are supported by detailed experiments.

1 Introduction

Optimization plays a fundamental role in the performance of machine learning models. The core problem it addresses is the minimization of the following optimization problem:

$$\min_{x \in \mathbb{R}^d} \left[f(x) := \frac{1}{N} \sum_{i=1}^N f_i(x) \right], \quad (1)$$

where $f, f_i : \mathbb{R}^d \rightarrow \mathbb{R}$ for $i = 1, \dots, N$. In machine learning, f is an empirical risk (or loss) function where f_i are the contributions due to the i -th data point. In this notation, $x \in \mathbb{R}^d$ is a vector of trainable parameters and N is the size of the dataset.

Solving Eq. (1) is typically achieved via Gradient Descent (GD) methods that, starting from a given estimate x_0 , iteratively update an estimate x_k as follows,

$$x_{k+1} = x_k - \eta \nabla f(x_k), \quad (2)$$

where $\eta > 0$ is the step size.

Since $\nabla f(x)$ requires computing the average of the N gradients $\nabla f_i(x)$ (which is computationally expensive for large datasets where $N \gg 1$), it is common to instead replace $\nabla f(x_k)$ with a gradient estimated on a subset of the dataset called a *mini-batch*. The resulting algorithm is known as Stochastic Gradient Descent (SGD) whose update is

$$x_{k+1} = x_k - \eta \nabla f_{\gamma_k}(x_k), \quad (3)$$

where $\{\gamma_k\}$ are i.i.d. random variables uniformly distributed and taking value in $\{1, \dots, N\}$.

Recently, Foret et al. (2020) proposed a stochastic optimizer known as Sharpness-Aware Minimization (SAM), which yields significant performance gains in various fields such as computer vision and natural language processing (Bahri et al., 2021; Foret et al., 2020). The general idea behind SAM is to seek parameters in low-loss regions that have a flatter curvature, which has been shown to improve the generalization of the model (Hochreiter and Schmidhuber, 1997; Keskar et al., 2016; Dziugaite and Roy, 2017; Jiang et al., 2019). The iteration of SAM is defined as

$$x_{k+1} = x_k - \eta \nabla f_{\gamma_k} \left(x_k + \rho \frac{\nabla f_{\gamma_k}(x_k)}{\|\nabla f_{\gamma_k}(x_k)\|} \right), \quad (4)$$

where $\rho > 0$ and $\{\gamma_k\}$ are i.i.d. random variables uniformly distributed and taking value in $\{1, \dots, N\}$. Numerous works have studied SAM and proposed variants such as ESAM (Du et al., 2021), ASAM (Kwon et al., 2021) and USAM (Andriushchenko and Flammarion, 2022). We will pay specific attention to the latter variant that drops the gradient normalization in Eq. (4), which yields the following update:

$$x_{k+1} = x_k - \eta \nabla f_{\gamma_k} (x_k + \rho \nabla f_{\gamma_k}(x_k)), \quad (5)$$

where $\rho > 0$ and $\{\gamma_k\}$ are i.i.d. random variables uniformly distributed and taking value in $\{1, \dots, N\}$. Following the theoretical framework of Li et al. (2017), our work provides the first *formal* derivation of the SDEs of SAM and USAM. Formally, such continuous-time models are weak approximations (i.e. approximations in distribution) of their respective discrete-time models. In this setup, they allow for gaining precious insights into the discrete-time dynamics (Su et al., 2014; Li et al., 2017).

In addition, we make the following contributions:

1. **Small ρ regime.** If $\rho = \mathcal{O}(\eta)$, we show that both SAM and USAM essentially behave like SGD.
2. **Moderate ρ regime.** For $\rho = \mathcal{O}(\sqrt{\eta})$, we derive an SDE model of USAM (9) and of SAM (12). Both can be interpreted as the SDE of SGD on an implicitly regularized loss and with an additional *implicit curvature-induced* noise. From the respective simplified versions of these SDEs (11) and (14), we demonstrate that the additional noise is driven by the Hessian of the loss so that the noise of the processes is larger in sharp minima. This is a key factor that leads USAM and SAM to prefer flatter minima where the additional noise decreases. However, while larger values of ρ increase the noise of the process, it also amplifies the implicit bias of the optimizer toward critical points independently of whether they are minima, saddles, or maxima.
3. **Empirical validation.** We empirically validate our results on several models and landscapes commonly studied in machine learning.

In order to gain further insights from the continuous-time models of SAM and USAM, we also study their behaviors on quadratic losses. The latter are commonly used to model the landscape in the proximity of a critical point (Ge et al., 2015; Levy, 2016; Jin et al., 2017; Poggio et al., 2017; Mandt et al., 2017b), including several recent works that studied SAM (Bartlett et al., 2022; Wen et al., 2022). This leads us to the following important observations:

1. **ODE - Pitfalls.** We derive precise conditions under which SAM and USAM converge to the origin even when it is a saddle or a maximum. To the best of our knowledge, this is the first time that these potential pitfalls have been revealed.
2. **SDE - Pitfalls.** We derive the stationary distribution of the USAM SDE and find that even this model is attracted by saddles under the same condition on ρ as found for the ODE¹. In contrast to

¹Of course, the SDE does not point-wise converge to the origin but rather oscillates around it with a certain variance.

USAM, we find that the dynamics of SAM is more complex: while a certain region centered at the origin behaves like an attractor, the origin itself repulses the dynamics away as the volatility rapidly increases to infinity.

3. **Empirical validation.** We empirically validate our claims for the quadratic loss as well as behavior in other models and landscapes as well.

Structure. The paper is organized as follows: In Section 2, we review related works and contextualize our work in the literature; in Section 3, we present the main theoretical results, i.e. the SDE of USAM and SAM. Then, we compare these SDEs to that of SGD and provide several novel insights about the behavior of USAM and SAM; in Section 4, we focus on quadratic losses and show that both the deterministic and stochastic versions of USAM and SAM can get attracted by saddles and maxima under certain conditions. Finally, we present our conclusions in Section 6. The proofs of our results and the details of the experiments are in the Appendix.

2 Related Work

Theoretical understanding of SAM The current understanding of the dynamics of SAM and USAM is still limited. Prior work includes the recent work by Bartlett et al. (2022) that shows that, for convex quadratics, SAM converges to a cycle oscillating between the sides of the minimum in the direction with the largest curvature. For the non-quadratic case, they also show that the dynamics drifts towards wider minima. A concurrent work by Wen et al. (2022) makes similar findings to Bartlett et al. (2022) as well as provides further insights regarding what notion of sharpness SAM regularizes. Additionally, Rangwani et al. (2022) showed that USAM could in some cases escape saddles faster than SGD, but we here provide a more complete description that shows that USAM can be much slower when it is close to a saddle.

ODE Approximations Continuous-time models in the form of (stochastic) differential equations are a well-established tool to study discrete-time optimizers; see e.g. Helmke and Moore (1994) and Kushner and Yin (2003). In machine learning, such models have lately received increasing interest to study both deterministic and stochastic optimizers. A notable reference is the work by Su et al. (2014) that derives a second-order ODE to model Nesterov’s accelerated gradient algorithm. ODE models have also been used recently to study SAM. This includes the work of Wen et al. (2022, Section 4.2) discussed above, as well as Andriushchenko and Flammarion (2022, Appendix B.1). Importantly we highlight two important differences with our work. First, our analysis focuses on the stochastic setting for which we derive SDEs. Second, the ODE representations used in these prior works only hold formally in the limit $\rho \rightarrow 0$, which is not the case in practical settings where $\rho > 0$. In contrast, our analysis allows for significantly larger values of ρ , more precisely $\rho = \mathcal{O}(\sqrt{\eta})$. Last but not least, neither of these papers empirically validates the ODEs they derived.

SDE Approximations of Stochastic Optimizers. For *stochastic* optimizers, Li et al. (2017, 2019) derived an SDE that provably approximates SGD (in the weak sense, i.e. in distribution). The validity of this SDE model was experimentally tested in Li et al. (2021). Similar results are derived for RMSprop and Adam by Malladi et al. (2022). In this paper, we derive an SDE approximation for SAM and USAM.

The proof technique employed in our work (as well as in Malladi et al. (2022)) relies on the theoretical framework established by Li et al. (2017, 2019). SDE approximations have also been derived for different types of noise. This includes heavy-tailed noise that is shown to be a good model for the noise of SGD in Simsekli et al. (2019) (although the evidence is still somewhat contested (Panigrahi et al., 2019; Xie et al., 2020; Li et al., 2021)). Zhou et al. (2020) also derived a Lévy-driven stochastic differential equation to model the non-gaussianity of the noise, which however does not enjoy any type of known theoretical

approximation guarantee. Finally, fractional Brownian noise (a generalization of Brownian noise that allows for correlation) was considered by Lucchi et al. (2022).

Applications of SDE approximations. Continuous-time models are valuable analysis tools to study and design new optimization methods. For instance, one concrete application of such models is the use of *stochastic optimal control* to select the learning rate (Li et al., 2017, 2019) or the batch size (Zhao et al., 2022). In addition, *scaling rules* to adjust the optimization hyperparameters w.r.t. the batch size can be recovered from SDE models (Malladi et al., 2022). Apart from these algorithmic contributions, SDE approximation can be useful to better understand stochastic optimization methods. In this regard, Jastrzebski et al. (2017) analyzed the factors influencing the minima found by SGD, and Orvieto and Lucchi (2019) derived convergence bounds for mini-batch SGD and SVRG. Smith et al. (2020) used an SDE model to distinguish between "noise-dominated" and "curvature-dominated" regimes of SGD. Yet another example is the study of *escape times* of SGD from minima of different sharpness (Xie et al., 2021). Moreover, Li et al. (2020) and Kunin et al. (2021) studied the *dynamics* of the SDE approximation under some symmetry assumptions. Finally, SDEs can be studied through the lens of various tools in the field of stochastic calculus, e.g. the Fokker–Planck equation gives access to the stationary distribution of a stochastic process. Such tools are for instance valuable in the field of Bayesian machine learning (Mandt et al., 2017a).

3 Formal Statements & Insights: The SDEs of SAM and USAM

In this Section, we present two general formulations of the SDEs of USAM and SAM. Due to the technical nature of the analysis, we refer the reader to the Appendix for the complete formal statements and proofs. For didactic reasons, we provide simplified versions under mild additional assumptions in the main paper.

Definition 1 (Weak Approximation). *Let G denote the set of continuous functions $\mathbb{R}^d \rightarrow \mathbb{R}$ of at most polynomial growth, i.e. $g \in G$ if there exists positive integers $\kappa_1, \kappa_2 > 0$ such that $|g(x)| \leq \kappa_1(1 + |x|^{2\kappa_2})$, for all $x \in \mathbb{R}^d$. Then, we say that a continuous-time stochastic process $\{X_t : t \in [0, T]\}$ is an order α weak approximation of a discrete stochastic process $\{x_k : k = 0, \dots, N\}$ if for every $g \in G$, there exists a positive constant C , independent of η , such that*

$$\max_{k=0, \dots, N} |\mathbb{E}g(x_k) - \mathbb{E}g(X_{k\eta})| \leq C\eta^\alpha. \quad (6)$$

This definition comes from the field of numerical analysis of SDEs, see for example Mil'shtein (1986). Consider the case where $g(x) = \|x\|^j$, then Eq. (6) bounds the difference between the j -th moments of the discrete and the continuous process.

First of all, we remind the reader that the order 1 weak approximation SDE of SGD (see Li et al. (2017, 2019)) is given by

$$dX_t = -\nabla f(X_t)dt + \sqrt{\eta} \left(\Sigma^{\text{SGD}}(X_t) \right)^{\frac{1}{2}} dW_t \quad (7)$$

where $\Sigma^{\text{SGD}}(x)$ is the SGD covariance matrix defined as

$$\Sigma^{\text{SGD}}(x) := \mathbb{E} \left[(\nabla f(x) - \nabla f_\gamma(x)) (\nabla f(x) - \nabla f_\gamma(x))^T \right]. \quad (8)$$

In Theorem 14 (USAM) and Theorem 19 (SAM), we prove that if $\rho = \mathcal{O}(\eta)$ (small ρ regime), the SDE of SGD is also an order 1 weak approximation for both USAM and SAM. In contrast, in the more realistic moderate ρ regime where $\rho = \mathcal{O}(\sqrt{\eta})$, Eq. (7) is no longer an order 1 weak approximation for either USAM or SAM. Under such a condition, we recover more insightful SDEs.

3.1 USAM SDE

Theorem 1 (USAM SDE - Informal Statement of Theorem 11). *Under sufficient regularity conditions and $\rho = \mathcal{O}(\sqrt{\eta})$ the solution of the following SDE is an order 1 weak approximation of the discrete update of USAM (5):*

$$dX_t = -\nabla \tilde{f}^{USAM}(X_t)dt + \sqrt{\eta} (\Sigma^{SGD}(X_t) + \rho (\Sigma^*(X_t) + \Sigma^*(X_t)^\top))^{1/2} dW_t \quad (9)$$

where $\Sigma^{SGD}(x)$ is given by Eq. (8) while

$$\Sigma^*(x) := \mathbb{E} \left[(\nabla f(x) - \nabla f_\gamma(x)) (\mathbb{E} [\nabla^2 f_\gamma(x) \nabla f_\gamma(x)] - \nabla^2 f_\gamma(x) \nabla f_\gamma(x))^\top \right] \quad (10)$$

and

$$\tilde{f}^{USAM}(x) := f(x) + \frac{\rho}{2} \mathbb{E} [\|\nabla f_\gamma(x)\|_2^2].$$

To have a more direct comparison with the SDE of SGD (Eq. (7)), we prove Corollary 2, a consequence of Theorem 1 that provides a more interpretable SDE for USAM.

Corollary 2 (Informal Statement of Corollary 13). *Under the assumptions of Theorem (1) and assuming a constant gradient noise covariance, i.e. $\nabla f_\gamma(x) = \nabla f(x) + Z$ such that Z is a noise vector that does not depend on x , the solution of the following SDE is the order 1 weak approximation of the discrete update of USAM (5):*

$$dX_t = -\nabla \tilde{f}^{USAM}(X_t)dt + (I + \rho \nabla^2 f(X_t)) (\eta \Sigma^{SGD}(X_t))^{1/2} dW_t \quad (11)$$

where $\Sigma^{SGD}(x)$ is given by Eq. (8) and

$$\tilde{f}^{USAM}(x) := f(x) + \frac{\rho}{2} \|\nabla f(x)\|_2^2.$$

Corollary 2 shows that the dynamics of USAM is equivalent to that of SGD on a regularized loss and with an additional noise component that depends on the curvature of the landscape (captured by the term $\nabla^2 f$). We comment in detail on these aspects in Section 3.3.

3.2 SAM SDE

Theorem 3 (SAM SDE - Informal Statement of Theorem 16). *Under sufficient regularity conditions and $\rho = \mathcal{O}(\sqrt{\eta})$ the solution of the following SDE is the order 1 weak approximation of the discrete update of SAM (4):*

$$dX_t = -\nabla \tilde{f}^{SAM}(X_t)dt + \sqrt{\eta} (\Sigma^{SGD}(X_t) + \rho (\Sigma^{**}(X_t) + \Sigma^{**}(X_t)^\top))^{1/2} dW_t \quad (12)$$

where $\Sigma^{SGD}(x)$ is given by Eq. (8) while

$$\Sigma^{**}(x) := \mathbb{E} \left[(\nabla f(x) - \nabla f_\gamma(x)) \left(\mathbb{E} \left[\frac{\nabla^2 f_\gamma(x) \nabla f_\gamma(x)}{\|\nabla f_\gamma(x)\|_2} \right] - \frac{\nabla^2 f_\gamma(x) \nabla f_\gamma(x)}{\|\nabla f_\gamma(x)\|_2} \right)^\top \right] \quad (13)$$

and

$$\tilde{f}^{SAM}(x) := f(x) + \rho \mathbb{E} [\|\nabla f_\gamma(x)\|_2].$$

To have a more direct comparison with the SDE of SGD (Eq. (7)), we derive a corollary of Theorem 3 that provides a more insightful SDE for SAM.

Corollary 4 (Informal Statement of Corollary 18). *Under the assumptions of Theorem 3 and assuming a constant gradient noise covariance, i.e. $\nabla f_\gamma(x) = \nabla f(x) + Z$ such that Z is a noise vector that does not depend on x , the solution of the following SDE is an order 1 weak approximation of the discrete update of SAM (4):*

$$dX_t = -\nabla \tilde{f}^{SAM}(X_t)dt + \left(I + \rho \frac{\nabla^2 f(X_t)}{\|\nabla f(X_t)\|} \right) (\eta \Sigma^{SGD}(X_t))^{1/2} dW_t \quad (14)$$

where $\Sigma^{SGD}(x)$ is given by Eq. (8) and

$$\tilde{f}^{SAM}(x) := f(x) + \rho \|\nabla f(x)\|_2.$$

Corollary 4 shows that similarly to USAM, the dynamics of SAM is equivalent to that of SGD on a regularized loss with an additional noise component that depends on the curvature of the landscape. However, we notice that, unlike USAM, the volatility component explodes near critical points. We elaborate on this later in Section 3.3.

3.3 Comparison: USAM vs SAM

The analyses of USAM and SAM (Eq. (11) and Eq. (14)) reveal that both algorithms are implicitly minimizing a regularized loss with an additional injection of noise (in addition to the SGD noise). While the regularized loss is $\frac{\rho}{2} \|\nabla f(x)\|_2^2$ for USAM, it is $\rho \|\nabla f(x)\|_2$ (not squared) for SAM. Therefore, when the process is closer to a stationary point, the regularization is stronger for SAM while it is the opposite when it is far away.

Regarding the additional noise, we observe that it is *curvature-dependent* as the Hessian appears in the expression of both volatility terms. Note that the sharper the minimum, the larger the noise contribution from the Hessian. This phenomenon is even more extreme for SAM where the volatility is scaled by the inverse of the norm of the gradient which drives the volatility to explode as it approaches a critical point. Intuitively, both SAM and USAM are more likely to stop or oscillate in a flat basin and more likely to escape from sharp minima than SGD.

We conclude with a discussion of the role of ρ . On one hand, larger values of ρ increase the variance of the process. On the other hand, it also increases the marginal importance of the factor $\frac{\rho}{2} \|\nabla f(x)\|_2^2$ (USAM) and $\rho \|\nabla f(x)\|_2$ (SAM), which for sufficiently large ρ might overshadow the marginal relevance of minimizing f and thus implicitly bias the optimizer toward any point with zero gradients, including saddles and maxima. We study this pitfall in detail for the quadratic case in the next Section and verify it experimentally in Section 5 for other models as well.

4 Behavior of SAM and USAM near saddles

In this Section, we leverage the ODEs (modeling the full-batch algorithms) and SDEs (modeling the mini-batch algorithms) to study the behavior of SAM and USAM near critical points. We especially focus on saddle points that have been a subject of significant interest in machine learning (Jin et al., 2017, 2021; Daneshmand et al., 2018). We consider a quadratic loss (which as mentioned earlier is a common model to study saddle points) of the form $f(x) = \frac{1}{2} x^\top H x$. W.l.o.g. we assume that the Hessian matrix H is diagonal² and denote the eigenvalues of H by $(\lambda_1, \dots, \lambda_d)$ where $\lambda_1 \geq \lambda_2 \geq \dots \geq \lambda_d$. If there are negative eigenvalues, we denote by λ_* the largest negative eigenvalue.

²Recall that symmetric matrices can be diagonalized.

4.1 USAM ODE

We study the deterministic dynamics of USAM defined as

$$dX_t = -H(X_t + \rho H X_t) = -H(I + \rho H)X_t, \implies X_t^j = X_0^j e^{-\lambda_j(1+\rho\lambda_j)t}. \quad (15)$$

Therefore, it is obvious (see Lemma 21) that, if all the eigenvalues of H are positive, for all $\rho > 0$, we have that $X_t^j \xrightarrow{t \rightarrow \infty} 0, \forall j \in \{1, \dots, d\}$. In particular, we notice that, since $e^{-\lambda_j(1+\rho\lambda_j)t} < e^{-\lambda_j t}$, such convergence to 0 is faster for the flow of USAM than for the gradient flow. More interestingly, if ρ is *too large*, the following result states that the deterministic dynamics of USAM might be attracted by a saddle or even a maximum.

Lemma 5 (Informal Statement of Lemma 22). *Let H have at least one strictly negative eigenvalue. Then, for all $\rho > -\frac{1}{\lambda_*}$,*

$$X_t^j \xrightarrow{t \rightarrow \infty} 0, \quad \forall j \in \{1, \dots, d\}. \quad (16)$$

Therefore, if ρ is not chosen appropriately, USAM might converge to $0 \in \mathbb{R}^d$, even if it is a saddle point or a maximum. Or course, we observe that if $\rho < \frac{1}{\lambda_*}$, USAM will not converge to the saddle (or maximum). However, we also notice that while it will escape it, since $e^{-\lambda_j(1+\rho\lambda_j)t} < e^{-\lambda_j t}$, it will do so slower than the gradient flow.

4.2 USAM SDE

Based on Corollary 13 and assuming $\Sigma^{\text{SGD}} = \varsigma^2 I$, the SDE of USAM is given by

$$dX_t = -H(I + \rho H)X_t dt + [(I + \rho H)\sqrt{\eta}\varsigma] dW_t. \quad (17)$$

Theorem 6 (Stationary distribution - Theorem 23 and Theorem 24). *If all the eigenvalues of H are positive, i.e. 0 is the minimum, we have that for any $\rho > 0$, the stationary distribution of Eq. (17) is*

$$P(x, \infty | \rho) = \sqrt{\frac{2\lambda_i}{\pi\eta\varsigma^2} \frac{1}{1 + \rho\lambda_i}} \exp\left[-\frac{2\lambda_i}{\eta\varsigma^2} \frac{1}{1 + \rho\lambda_i} x^2\right], \quad \forall i \in \{1, \dots, d\}. \quad (18)$$

If there exists a negative eigenvalue, this formula does not, in general, parametrize a probability distribution. However, if $\rho > -\frac{1}{\lambda_}$, Eq. (18) is still the stationary distribution of Eq.(17), $\forall i \in \{1, \dots, d\}$.*

Theorem 6 states that in case the origin is a saddle (or a maximum) and ρ is small enough, the stationary distribution of USAM is divergent at infinity, meaning that the process will escape the bad critical point. In such a case, the escape from the saddle is slower than SGD as the variance in the direction of negative eigenvalues, e.g. the escape directions, is smaller. However, if ρ is too large, then the dynamics of the USAM SDE will oscillate around the origin even if this is a saddle or a maximum. This is consistent with the results derived for the ODE of USAM in Section 4.1. There, we found that under the very same condition on ρ , the dynamics of the USAM SDE converges to 0 even when it is a saddle or a maximum.

4.3 SAM ODE

Let us recall that the ODE of SAM for the quadratic loss is given by

$$dX_t = -H \left(I + \frac{\rho H}{\|H X_t\|} \right) X_t, \quad (19)$$

where w.l.o.g. we take H to be a diagonal matrix.

Lemma 7 (Lemma 26). *For all $\rho > 0$, if H is PSD (Positive Semi-Definite), the origin is (locally) asymptotically stable. Additionally, if H is not PSD and $\|HX_t\| \leq -\rho\lambda_*$, then the origin is still (locally) asymptotically stable.*

Lemma 7 demonstrates that USAM and SAM have completely different behaviors. For USAM, Lemma 5 shows that selecting ρ small enough would prevent the convergence towards a saddle or a maximum. In contrast, Lemma 7 shows that for any value of ρ , if the dynamics of SAM is close enough to any critical point, i.e. enters an attractor, it is attracted by it. We also observe that if $\rho \rightarrow 0$, this attractor reduces to a single point, i.e. the critical point itself.

Finally, by comparing Eq. (15) with Eq. (19), we observe that the dynamics of SAM is equivalent to that of USAM where the radius ρ has been scaled by $\frac{1}{\|HX_t\|}$. In a way, while USAM has a fixed radius ρ , SAM has an *time-dependent* radius $\frac{\rho}{\|HX_t\|}$ which is smaller than ρ if the dynamics is far from the origin ($\|HX_t\| > 1$) and larger when it is close to it ($\|HX_t\| < 1$). Therefore, SAM converges to the origin slower than USAM when it is far from it and it becomes faster and faster the closer it gets. To the best of our knowledge, these insights have not been observed before and might have important practical consequences.

4.4 SAM SDE

We remind the reader, that based on Corollary 18, the SDE of SAM for the quadratic loss is given by

$$dX_t = -H \left(I + \frac{\rho H}{\|HX_t\|} \right) X_t + \sqrt{\eta} \varsigma \left(I + \frac{\rho H}{\|HX_t\|} \right) dW_t \quad (20)$$

Observation 8 (Details in 27). *We observe that for all $\rho > 0$, there exists an $\epsilon > 0$ such that if $\|HX_t\| \in (\epsilon, -\rho\lambda_*)$, the dynamics of X_t is attracted towards the origin. If the eigenvalues are all positive, the condition becomes $\|HX_t\| \in (\epsilon, \infty)$. On the contrary, if $\|HX_t\| < \epsilon$, then the dynamics is pushed away from the origin.*

This insight suggests that if SAM is initialized close enough to a quadratic saddle, it is attracted toward it, but is also repulsed by it if it gets too close. This is due to the explosion of the volatility next to the origin. In the next Section, we experimentally verify that the dynamics gets cyclically pulled to 0 and pushed away from it, not only for the quadratic saddle but also for that of other models.

5 Experiments

In this Section, we experimentally verify the validity of Corollary 2 and Corollary 4. Then, we validate the insights drawn from the SAM SDE presented in Section 4.4. Finally, we study the behavior of SAM near saddle points, checking the effect as it is initialized closer and closer to a saddle in non-quadratic models.

5.1 Empirical Validation of SDEs for USAM and SAM

We first experimentally validate the results of Corollary 2 and Corollary 4. To do so, we use two different test functions ($g(x)$ in Eq. (6)), which are $g_1(x) := \|x\| + \|\nabla f(x)\|$ and $g_2(x) := f(x)$ on three models of increasing complexity. Figure 1 uses the first metric $g_1(x)$ to measure the maximum absolute error (across the whole trajectory) of the SDEs of SGD, USAM, and SAM in approximating the respective discrete algorithms. Additionally, we plot the same error if we were to use the SDE of SGD to model/approximate the discrete iterates of USAM and SAM. We observe that when $\rho = \eta$, the absolute error is small in all

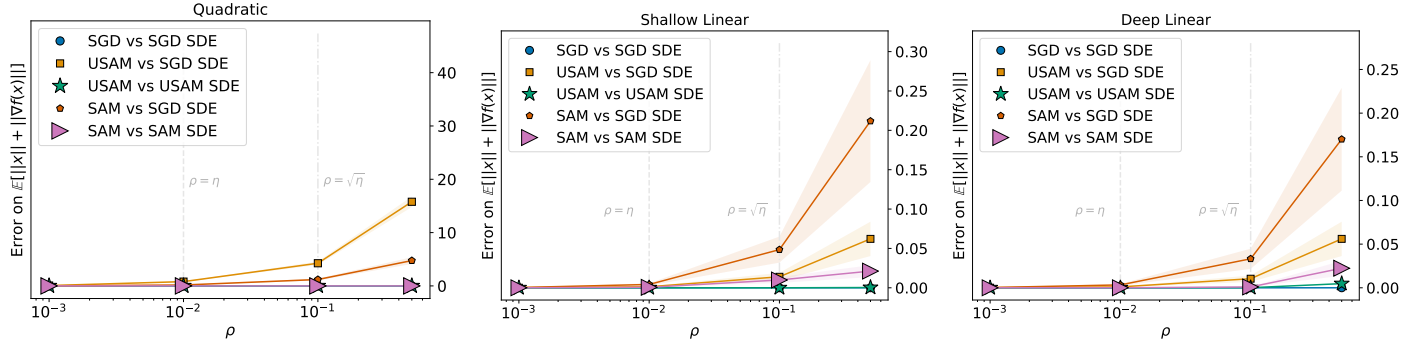


Figure 1: Comparison with respect to $g_1(x)$ with respect to ρ - Quadratic (left); Shallow linear class (center); Deep linear class (right).

cases, meaning that all the discrete iterates and SDEs behave essentially in the same way. This supports our claim that if $\rho = \mathcal{O}(\eta)$, the SDE of SGD is a good model for USAM and SAM as well (Theorem 14 and Theorem 19). When $\rho = \sqrt{\eta}$, we see that the SDEs of USAM and SAM correctly approximate the respective discrete algorithms, while the SDE of SGD has a significantly larger relative error, which validates the results of Corollary 2 and Corollary 4. Although we do not have any theoretical guarantee for larger ρ , we observe empirically that the modeling error is still rather low. Finally, Figure 2 shows the evolution of the metric $g_2(x) := f(x)$ for the different algorithms. We notice that all the SDEs are matching the respective algorithms. More details are in the Appendix C.1.

Interplay between noise, curvature, ρ , and suboptimality Next, we check how the parameter ρ and the curvature (measured by the trace operator of the Hessian) influence the noise of the stochastic process and its suboptimality. These insights substantiate the intuition that USAM and SAM are more likely to escape sharp minima faster than SGD.

First of all, we fix the value of ρ as well as a diagonal Hessian H with random positive eigenvalues. Then, we study the loss for SGD, USAM, and SAM as they optimize a convex quadratic loss of increasingly larger curvature (i.e. larger Hessian magnitude). The left of Figure 5 in Appendix shows that SAM exhibits a larger loss with more variance, and even more so as the curvature increases. In the middle image, we observe that in line with Jastrzebski et al. (2017), the noise of the loss of SGD increases linearly with the trace of the Hessian. On the right of Figure 5 in Appendix, we see that, as expected, SAM exhibits a loss that is orders of magnitude larger than SGD and with much more variance. Similar observations can be done for USAM, see Figure 6 in Appendix.

In a similar experiment, we fix the Hessian as above and study the loss as we increase ρ . Once again, we see on the left of Figure 7 in Appendix that SAM exhibits a larger loss with more variance, and this is more and more clear as ρ increases. Similar observations can be done for USAM in Figure 8 in Appendix.

We conclude that indeed both USAM and SAM have an implicit curvature-induced noise additional to that of SGD which leads to increased suboptimality as well as a higher likelihood to escape sharp minima than SGD. We provide an additional theoretical justification for this phenomenon in Observation 25.

5.2 Behavior of SAM and USAM near Saddles

In this Section, we study the behavior of SAM and USAM near saddles. We refer to SAM and USAM as their full-batch versions, PSAM and PUSAM when we perturb their gradients (with Gaussian noise).

Quadratic Landscape We first empirically verify the insight gained in Section 4.4 — the dynamics is attracted to the origin, but if it gets too close, it gets repulsed away. For a quadratic saddle, in Figure 3 we show the distribution of 10^5 trajectories after $5 \cdot 10^4$ iterations. These are distributed symmetrically

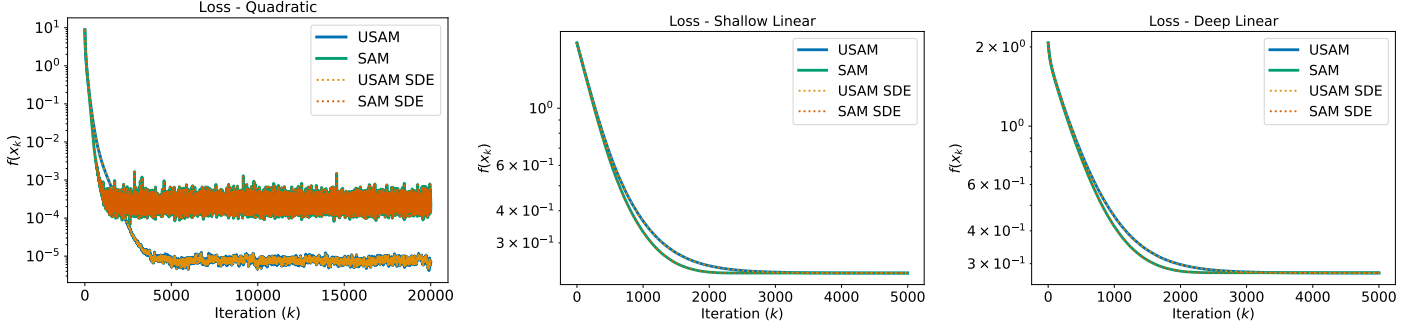


Figure 2: Comparison with respect to $g_2(x)$ with respect to time - Quadratic (left); Shallow linear class (center); Deep linear class (right).

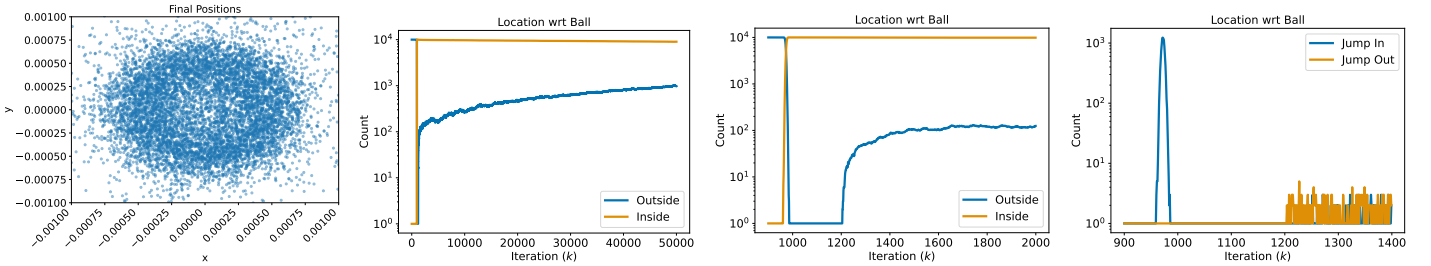


Figure 3: Quadratic Saddle - Left: Distribution points around the origin is scarcer near to the origin; Center-Left: Number of trajectories outside a small ball around the origin increases over time; Center-Right: All the trajectories eventually enter the ball and then start exiting it; Right: There is a constant oscillation of points in and out of the ball.

around the origin but the concentration is lower close to it. While this is intuitive for the convex case (see Figure 9 in Appendix), it is surprising for the saddle case, and our insights are fully verified. The second and third images of Figure 3 show that all the trajectories are initialized outside of a certain ball around the origin and then they get pulled inside it. Then, we see that the number of points outside this ball increased again and the right-most image shows the number of points jumping in and out of it. This shows that there is a cyclical dynamics towards and away from the origin. Of course, all the points eventually escape the saddle, but much more slowly than what would happen under the dynamics of SGD where the trajectories would not even get close to the origin in the first place. In Figure 10 in Appendix, we show the behavior of several optimizers when initialized in an escaping direction from the saddle and we observe that full-batch SAM is attracted by the saddle while the others are able to escape it. Interestingly, PSAM is the slowest stochastic model to escape. Figure 10 in Appendix shows that full-batch SAM cannot escape the saddle if it is too close to it, while PSAM can if it is close enough to enjoy a spike in volatility. More details are in the Appendix C.2.

Linear Autoencoder Inspired by the insights gained so far, we study the behavior of SAM when it is initialized close to the saddle present at the origin of the linear autoencoder introduced by Kunin et al. (2019). The left of Figure 4 shows the evolution of the loss as we optimize it with SAM starting from different starting points closer and closer to the saddle in the origin. The scalar σ parametrizes how close the initialization is to the origin. We observe that when SAM starts sufficiently far from it ($\sigma \geq 0.005$), it optimizes immediately, while the closer it is initialized to it, the more it stays around it, up to not being able to move at all ($\sigma \leq 0.001$). Regarding PSAM, in the middle figure, we observe the same behavior, apart from one case: if it is initialized sufficiently close to the origin, instead of getting stuck there, it jumps away following a spike in volatility. The right of Figure 4 shows the comparison with other optimizers:

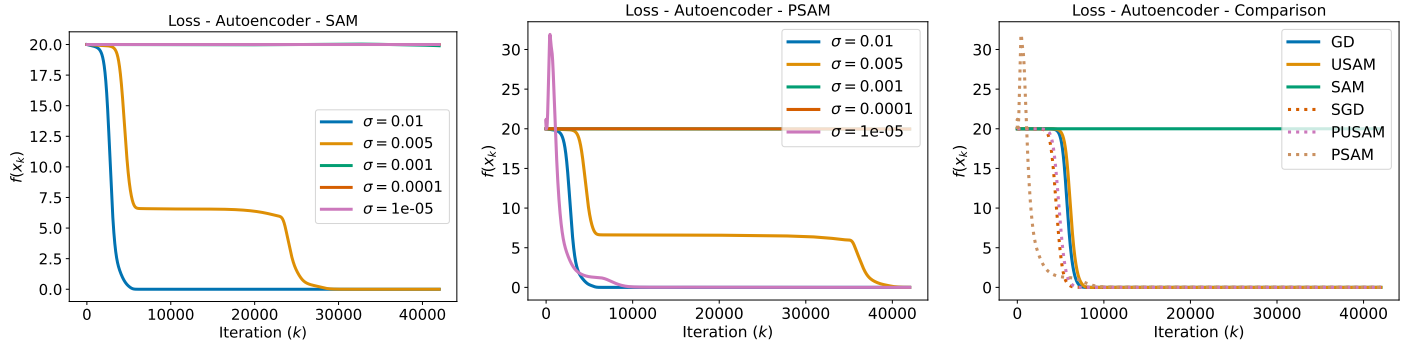


Figure 4: Autoencoder - Left: SAM does not escape the saddle if it is too close to it. Center: PSAM escapes if it is extremely close to the origin thanks to a volatility spike. Right: PSAM is the fastest to escape, while SAM is stuck.

SAM does not optimize the loss while the other optimizers do. These findings are consistent with those observed in Figure 10 in Appendix for the quadratic landscape. In Figure 11 in Appendix, we show a similar result for a saddle landscape studied in Lucchi et al. (2022). More details are in Appendix C.3 and Appendix C.4, respectively. In both these experiments, we observe the suboptimality patterns forecasted by our theory.

6 Conclusion

We proposed new continuous-time models (in the form of SDEs) for the SAM optimizer and its unnormalized variant USAM. We formally proved (and experimentally verified) that these SDEs approximate the real discrete-time optimizers SAM and USAM; see Theorems 1–4 for the theory and Section 5.1 for the experiments.

These SDEs thus describe the dynamics of SAM and USAM in the parameter space of an optimization problem. Notably, they explicitly decompose these dynamics into a deterministic drift and a stochastic diffusion coefficient which in itself reveals some novel insights: The drift coefficient – by the definition of f in Theorems 1–4 – exposes how the ascent parameter ρ impacts the average dynamics of SAM and USAM. The diffusion coefficient, on the other hand, increases with the Hessian of the loss – thereby implying that SAM and USAM are noisier in sharp minima. This could be interpreted as an implicit bias towards flat minima (as sharp minima will be more unstable due to the noise).

The continuous-time SDE models allow the application of tools from stochastic calculus (e.g. integration and differentiation) to study the behavior of SAM and USAM. As a start in this direction, we proved that the flow of USAM gets stuck around saddles if ρ is too large. In contrast, SAM oscillates around saddles if initialized close to them but eventually slowly escapes them thanks to the additional noise. Importantly, our claims are substantiated by experiments on several models and invite further investigation to prevent a costly waste of computation budget near saddle points.

Finally, we expect that the application of more analytical tools to the SDEs will lead to further insights into SAM in future work. It would for instance be of particular interest to revisit claims made about other optimizers via their SDE models (see “Applications of SDE approximations” in Section 2). Hopefully, this will help to demystify the high performance of SAM on large-scale ML problems.

Acknowledgement This work was supported in part by the Swiss National Foundation, SNF grant No 207392.

References

Maksym Andriushchenko and Nicolas Flammarion. Towards understanding sharpness-aware minimization. In *International Conference on Machine Learning*, pages 639–668. PMLR, 2022.

Dara Bahri, Hossein Mobahi, and Yi Tay. Sharpness-aware minimization improves language model generalization. *arXiv preprint arXiv:2110.08529*, 2021.

Peter L Bartlett, Philip M Long, and Olivier Bousquet. The dynamics of sharpness-aware minimization: Bouncing across ravines and drifting towards wide minima. *arXiv preprint arXiv:2210.01513*, 2022.

Hadi Daneshmand, Jonas Kohler, Aurelien Lucchi, and Thomas Hofmann. Escaping saddles with stochastic gradients. In *International Conference on Machine Learning*, pages 1155–1164. PMLR, 2018.

Jiawei Du, Hanshu Yan, Jiashi Feng, Joey Tianyi Zhou, Liangli Zhen, Rick Siow Mong Goh, and Vincent YF Tan. Efficient sharpness-aware minimization for improved training of neural networks. *arXiv preprint arXiv:2110.03141*, 2021.

Dheeru Dua and Casey Graff. UCI machine learning repository, 2017. URL <http://archive.ics.uci.edu/ml>.

Gintare Karolina Dziugaite and Daniel M Roy. Computing nonvacuous generalization bounds for deep (stochastic) neural networks with many more parameters than training data. *arXiv preprint arXiv:1703.11008*, 2017.

Gerald B Folland. Higher-order derivatives and taylor’s formula in several variables. *Preprint*, pages 1–4, 2005.

Pierre Foret, Ariel Kleiner, Hossein Mobahi, and Behnam Neyshabur. Sharpness-aware minimization for efficiently improving generalization. *arXiv preprint arXiv:2010.01412*, 2020.

Crispin W Gardiner et al. *Handbook of stochastic methods*, volume 3. Springer Berlin, 1985.

Rong Ge, Furong Huang, Chi Jin, and Yang Yuan. Escaping from saddle points—online stochastic gradient for tensor decomposition. In *Conference on Learning Theory*, pages 797–842, 2015.

Uwe Helmke and John B Moore. *Optimization and Dynamical Systems*. Springer London, 1st edition, 1994.

Sepp Hochreiter and Jürgen Schmidhuber. Flat minima. *Neural computation*, 9(1):1–42, 1997.

Stanisław Jastrzebski, Zachary Kenton, Devansh Arpit, Nicolas Ballas, Asja Fischer, Yoshua Bengio, and Amos Storkey. Three factors influencing minima in sgd. *arXiv preprint arXiv:1711.04623*, 2017.

Yiding Jiang, Behnam Neyshabur, Hossein Mobahi, Dilip Krishnan, and Samy Bengio. Fantastic generalization measures and where to find them. In *International Conference on Learning Representations*, 2019.

Chi Jin, Rong Ge, Praneeth Netrapalli, Sham M Kakade, and Michael I Jordan. How to escape saddle points efficiently. In *International Conference on Machine Learning*, pages 1724–1732. PMLR, 2017.

Chi Jin, Praneeth Netrapalli, Rong Ge, Sham M. Kakade, and Michael I. Jordan. On nonconvex optimization for machine learning: Gradients, stochasticity, and saddle points. *J. ACM*, 68(2), 2021.

Nitish Shirish Keskar, Dheevatsa Mudigere, Jorge Nocedal, Mikhail Smelyanskiy, and Ping Tak Peter Tang. On large-batch training for deep learning: Generalization gap and sharp minima. *arXiv preprint arXiv:1609.04836*, 2016.

Daniel Kunin, Jonathan Bloom, Aleksandrina Goeva, and Cotton Seed. Loss landscapes of regularized linear autoencoders. In *International Conference on Machine Learning*, pages 3560–3569. PMLR, 2019.

Daniel Kunin, Javier Sagastuy-Brena, Surya Ganguli, Daniel LK Yamins, and Hidenori Tanaka. Neural mechanics: Symmetry and broken conservation laws in deep learning dynamics. In *International Conference on Learning Representations*, 2021.

Harold Kushner and G George Yin. *Stochastic approximation and recursive algorithms and applications*, volume 35. Springer Science & Business Media, 2003.

Jungmin Kwon, Jeongseop Kim, Hyunseo Park, and In Kwon Choi. Asam: Adaptive sharpness-aware minimization for scale-invariant learning of deep neural networks. In *International Conference on Machine Learning*, pages 5905–5914. PMLR, 2021.

Kfir Y Levy. The power of normalization: Faster evasion of saddle points. *arXiv preprint arXiv:1611.04831*, 2016.

Qianxiao Li, Cheng Tai, and E Weinan. Stochastic modified equations and adaptive stochastic gradient algorithms. In *International Conference on Machine Learning*, pages 2101–2110. PMLR, 2017.

Qianxiao Li, Cheng Tai, and E Weinan. Stochastic modified equations and dynamics of stochastic gradient algorithms i: Mathematical foundations. *The Journal of Machine Learning Research*, 20(1):1474–1520, 2019.

Zhiyuan Li, Kaifeng Lyu, and Sanjeev Arora. Reconciling modern deep learning with traditional optimization analyses: the intrinsic learning rate. In *Advances in Neural Information Processing Systems*, 2020.

Zhiyuan Li, Sadhika Malladi, and Sanjeev Arora. On the validity of modeling SGD with stochastic differential equations (SDEs). In A. Beygelzimer, Y. Dauphin, P. Liang, and J. Wortman Vaughan, editors, *Advances in Neural Information Processing Systems*, 2021.

Aurelien Lucchi, Frank Proske, Antonio Orvieto, Francis Bach, and Hans Kersting. On the theoretical properties of noise correlation in stochastic optimization. In *Advances in Neural Information Processing Systems*, 2022.

Sadhika Malladi, Kaifeng Lyu, Abhishek Panigrahi, and Sanjeev Arora. On the SDEs and scaling rules for adaptive gradient algorithms. In *Advances in Neural Information Processing Systems*, 2022.

Stephan Mandt, Matthew D. Hoffman, and David M. Blei. Stochastic gradient descent as approximate Bayesian inference. *J. Mach. Learn. Res.*, 18(1):4873–4907, 2017a. ISSN 1532-4435.

Stephan Mandt, Matthew D Hoffman, and David M Blei. Stochastic gradient descent as approximate bayesian inference. *arXiv preprint arXiv:1704.04289*, 2017b.

Xuerong Mao. *Stochastic differential equations and applications*. Elsevier, 2007.

GN Mil'shtein. Weak approximation of solutions of systems of stochastic differential equations. *Theory of Probability & Its Applications*, 30(4):750–766, 1986.

Antonio Orvieto and Aurelien Lucchi. Continuous-time models for stochastic optimization algorithms. *Advances in Neural Information Processing Systems*, 32, 2019.

Abhishek Panigrahi, Raghav Somani, Navin Goyal, and Praneeth Netrapalli. Non-Gaussianity of stochastic gradient noise. *arXiv preprint arXiv:1910.09626*, 2019.

Tomaso Poggio, Kenji Kawaguchi, Qianli Liao, Brando Miranda, Lorenzo Rosasco, Xavier Boix, Jack Hidary, and Hrushikesh Mhaskar. Theory of deep learning iii: explaining the non-overfitting puzzle. *arXiv preprint arXiv:1801.00173*, 2017.

Harsh Rangwani, Sumukh K Aithal, Mayank Mishra, and R Venkatesh Babu. Escaping saddle points for effective generalization on class-imbalanced data. *arXiv preprint arXiv:2212.13827*, 2022.

Hannes Risken. Fokker-planck equation. In *The Fokker-Planck Equation*, pages 63–95. Springer, 1996.

Levent Sagun, Utku Evci, V Ugur Guney, Yann Dauphin, and Leon Bottou. Empirical analysis of the hessian of over-parametrized neural networks. *arXiv preprint arXiv:1706.04454*, 2017.

Umut Simsekli, Levent Sagun, and Mert Gurbuzbalaban. A tail-index analysis of stochastic gradient noise in deep neural networks. In *International Conference on Machine Learning*, 2019.

Samuel Smith, Erich Elsen, and Soham De. On the generalization benefit of noise in stochastic gradient descent. In *International Conference on Machine Learning*, 2020.

Weijie Su, Stephen Boyd, and Emmanuel Candes. A differential equation for modeling Nesterov's accelerated gradient method: Theory and insights. In *Advances in Neural Information Processing Systems*, 2014.

Kaiyue Wen, Tengyu Ma, and Zhiyuan Li. How does sharpness-aware minimization minimize sharpness? *arXiv preprint arXiv:2211.05729*, 2022.

Zeke Xie, Issei Sato, and Masashi Sugiyama. A diffusion theory for deep learning dynamics: Stochastic gradient descent exponentially favors flat minima. *arXiv preprint arXiv:2002.03495*, 2020.

Zeke Xie, Issei Sato, and Masashi Sugiyama. A diffusion theory for deep learning dynamics: Stochastic gradient descent exponentially favors flat minima. In *International Conference on Learning Representations*, 2021.

Jim Zhao, Aurelien Lucchi, Frank Norbert Proske, Antonio Orvieto, and Hans Kersting. Batch size selection by stochastic optimal control. In *Has it Trained Yet? NeurIPS 2022 Workshop*, 2022.

Pan Zhou, Jiashi Feng, Chao Ma, Caiming Xiong, Steven Chu Hong Hoi, et al. Towards theoretically understanding why sgd generalizes better than adam in deep learning. *Advances in Neural Information Processing Systems*, 33:21285–21296, 2020.

Zhanxing Zhu, Jingfeng Wu, Bing Yu, Lei Wu, and Jinwen Ma. The regularization effects of anisotropic noise in stochastic gradient descent. *ArXiv e-prints*, 2018.

A Theoretical Framework - SDEs

In the subsequent proofs, we will make repeated use of Taylor expansions in powers of η . To simplify the presentation, we introduce the shorthand that whenever we write $\mathcal{O}(\eta^\alpha)$, we mean that there exists a function $K(x) \in G$ such that the error terms are bounded by $K(x)\eta^\alpha$. For example, we write

$$b(x + \eta) = b_0(x) + \eta b_1(x) + \mathcal{O}(\eta^2)$$

to mean: there exists $K \in G$ such that

$$|b(x + \eta) - b_0(x) - \eta b_1(x)| \leq K(x)\eta^2.$$

Additionally, let us introduce some notation:

- A multi-index is $\alpha = (\alpha_1, \alpha_2, \dots, \alpha_n)$ such that $\alpha_j \in \{0, 1, 2, \dots\}$
- $|\alpha| := \alpha_1 + \alpha_2 + \dots + \alpha_n$
- $\alpha! := \alpha_1! \alpha_2! \dots \alpha_n!$
- For $x = (x_1, x_2, \dots, x_n) \in \mathbb{R}^n$, we define $x^\alpha := x_1^{\alpha_1} x_2^{\alpha_2} \dots x_n^{\alpha_n}$
- For a multi-index β , $\partial_\beta^{|\beta|} f(x) := \frac{\partial^{|\beta|}}{\partial_{x_1}^{\beta_1} \partial_{x_2}^{\beta_2} \dots \partial_{x_n}^{\beta_n}} f(x)$
- We also denote the partial derivative with respect to x_i by ∂_i .

Lemma 9 (Lemma 1 Li et al. (2017)). *Let $0 < \eta < 1$. Consider a stochastic process $X_t, t \geq 0$ satisfying the SDE*

$$dX_t = b(X_t) dt + \eta^{\frac{1}{2}} \sigma(X_t) dW_t$$

with $X_0 = x \in \mathbb{R}^d$ and b, σ together with their derivatives belong to G . Define the one-step difference $\Delta = X_\eta - x$, then we have

1. $\mathbb{E} \Delta_i = b_i \eta + \frac{1}{2} \left[\sum_{j=1}^d b_j \partial_j b_i \right] \eta^2 + \mathcal{O}(\eta^3) \quad \forall i = 1, \dots, d;$
2. $\mathbb{E} \Delta_i \Delta_j = \left[b_i b_j + \sigma \sigma_{(ij)}^T \right] \eta^2 + \mathcal{O}(\eta^3) \quad \forall i, j = 1, \dots, d;$
3. $\mathbb{E} \prod_{j=1}^s \Delta_{(ij)} = \mathcal{O}(\eta^3)$ for all $s \geq 3, i, j = 1, \dots, d$.

All functions above are evaluated at x .

Theorem 10 (Theorem 2 and Lemma 5, Mil'shtein (1986)). *Let the assumptions in Theorem 11 hold. If in addition there exists $K_1, K_2, K_3, K_4 \in G$ so that*

1. $|\mathbb{E}\Delta_i - \mathbb{E}\bar{\Delta}_i| \leq K_1(x)\eta^2, \quad \forall i = 1, \dots, d;$
2. $|\mathbb{E}\Delta_i\Delta_j - \mathbb{E}\bar{\Delta}_i\bar{\Delta}_j| \leq K_2(x)\eta^2, \quad \forall i, j = 1, \dots, d;$
3. $|\mathbb{E}\prod_{j=1}^s \Delta_{i_j} - \mathbb{E}\prod_{j=1}^s \bar{\Delta}_{i_j}| \leq K_3(x)\eta^2, \quad \forall s \geq 3, \quad \forall i_j \in \{1, \dots, d\};$
4. $\mathbb{E}\prod_{j=1}^3 |\bar{\Delta}_{i_j}| \leq K_4(x)\eta^2, \quad \forall i_j \in \{1, \dots, d\}.$

Then, there exists a constant C so that for all $k = 0, 1, \dots, N$ we have

$$|\mathbb{E}g(X_{k\eta}) - \mathbb{E}g(x_k)| \leq C\eta.$$

A.1 Formal Derivation - USAM

The next result is inspired by Theorem 1 of Li et al. (2017) and is derived under some regularity assumption on the function f .

Assumption 1. *Assume that the following conditions on f, f_i and their gradients are satisfied:*

- $\nabla f, \nabla f_i$ satisfy a Lipschitz condition: there exists $L > 0$ such that

$$|\nabla f(x) - \nabla f(y)| + \sum_{i=1}^n |\nabla f_i(x) - \nabla f_i(y)| \leq L|x - y|;$$

- f, f_i and its partial derivatives up to order 7 belong to G ;
- $\nabla f, \nabla f_i$ satisfy a growth condition: there exists $M > 0$ such that

$$|\nabla f(x)| + \sum_{i=1}^n |\nabla f_i(x)| \leq M(1 + |x|);$$

We will consider the stochastic process $X_t \in \mathbb{R}^d$ defined by

$$dX_t = -\nabla \tilde{f}^{\text{USAM}}(X_t)dt + \sqrt{\eta} \left(\Sigma^{\text{SGD}}(X_t) + \rho \left(\Sigma^*(X_t) + \Sigma^*(X_t)^\top \right)^{\frac{1}{2}} dW_t \right) \quad (21)$$

where

$$\Sigma^{\text{SGD}}(x) := \mathbb{E} \left[(\nabla f(x) - \nabla f_\gamma(x)) (\nabla f(x) - \nabla f_\gamma(x))^\top \right].$$

is the usual covariance of SGD, while

$$\Sigma^*(x) := \mathbb{E} \left[(\nabla f(x) - \nabla f_\gamma(x)) \left(\mathbb{E} [\nabla^2 f_\gamma(x) \nabla f_\gamma(x)] - \nabla^2 f_\gamma(x) \nabla f_\gamma(x) \right)^\top \right] \quad (22)$$

and

$$\tilde{f}^{\text{USAM}}(x) := f(x) + \frac{\rho}{2} \mathbb{E} [\|\nabla f_\gamma(x)\|_2^2].$$

In the following, we will use the notation

$$\Sigma^{\text{USAM}}(x) := (\Sigma^{\text{SGD}}(X_t) + \rho (\Sigma^*(X_t) + \Sigma^*(X_t)^\top)) \quad (23)$$

Theorem 11 (Stochastic modified equations). *Let $0 < \eta < 1, T > 0$ and set $N = \lfloor T/\eta \rfloor$. Let $x_k \in \mathbb{R}^d, 0 \leq k \leq N$ denote a sequence of SAM iterations defined by Eq. (5). Additionally, let us take*

$$\rho = \mathcal{O}\left(\eta^{\frac{1}{2}}\right). \quad (24)$$

Consider the stochastic process X_t defined in Eq. (21) and fix some test function $g \in G$ and suppose that g and its partial derivatives up to order 6 belong to G .

Then, under Assumption 1, there exists a constant $C > 0$ independent of η such that for all $k = 0, 1, \dots, N$, we have

$$|\mathbb{E}g(X_{k\eta}) - \mathbb{E}g(x_k)| \leq C\eta^1.$$

That is, the SDE (21) is an order 1 weak approximation of the SAM iterations (5).

Lemma 12. *Under the assumptions of Theorem 11, let $0 < \eta < 1$ and consider $x_k, k \geq 0$ satisfying the USAM iterations (5)*

$$x_{k+1} = x_k - \eta \nabla f_{\gamma_k}(x_k + \rho \nabla f_{\gamma_k}(x_k))$$

with $x_0 = x \in \mathbb{R}^d$. Additionally, we define $\partial_i \tilde{f}^{\text{USAM}}(x) := \partial_{e_i} f(x) + \rho \mathbb{E} \left[\sum_j \partial_{e_i+e_j}^2 f_\gamma(x) \partial_{e_j} f_\gamma(x) \right]$.

From the definition the one-step difference $\bar{\Delta} = x_1 - x$, then we have

1. $\mathbb{E} \bar{\Delta}_i = -\partial_i \tilde{f}^{\text{USAM}}(x) \eta + \mathcal{O}(\eta \rho^2) \quad \forall i = 1, \dots, d.$
2. $\mathbb{E} \bar{\Delta}_i \bar{\Delta}_j = \partial_i \tilde{f}^{\text{USAM}}(x) \partial_j \tilde{f}^{\text{USAM}}(x) \eta^2 + \Sigma_{(ij)}^{\text{SAM}} \eta^2 + \mathcal{O}(\eta^3) \quad \forall i, j = 1, \dots, d.$
3. $\mathbb{E} \prod_{j=1}^s \Delta_{i_j} = \mathcal{O}(\eta^3) \quad \forall s \geq 3, \quad i_j \in \{1, \dots, d\}.$

and all the functions above are evaluated at x .

Proof of Lemma 12. Since the first step is to evaluate $\mathbb{E} \Delta_i = \mathbb{E} [\partial_{e_i} f_\gamma(x + \rho \nabla f_\gamma(x)) \eta]$, we start by analyzing $\partial_{e_i} f_\gamma(x + \rho \nabla f_\gamma(x))$, that is the partial derivative in the direction $e_i := (0, \dots, 0, \underset{i\text{-th}}{1}, 0, \dots, 0)$. Then, we have that

$$\partial_{e_i} f_\gamma(x + \rho \nabla f_\gamma(x)) = \partial_{e_i} f_\gamma(x) + \sum_{|\alpha|=1} \partial_{e_i+\alpha}^2 f_\gamma(x) \rho \partial_\alpha f_\gamma(x) + \mathcal{R}_{x,1}^{\partial_{e_i} f_\gamma(x)}(\rho \nabla f_\gamma(x)), \quad (25)$$

where the residual is defined in Eq. (4) of Folland (2005). Therefore, for some constant $c \in (0, 1)$, it holds that

$$\mathcal{R}_{x,1}^{\partial_{e_i} f_\gamma(x)}(\rho \nabla f_\gamma(x)) = \sum_{|\alpha|=2} \frac{\partial_{e_i+\alpha}^3 f_\gamma(x + c\rho \nabla f_\gamma(x)) \rho^2 (\nabla f_\gamma(x))^\alpha}{\alpha!}. \quad (26)$$

Therefore, we can rewrite it as

$$\partial_{e_i} f_\gamma(x + \rho \nabla f_\gamma(x)) = \partial_{e_i} f_\gamma(x) + \rho \sum_j \partial_{e_i+e_j}^2 f_\gamma(x) \partial_{e_j} f_\gamma(x) + \rho^2 \left[\sum_{|\alpha|=2} \frac{\partial_{e_i+\alpha}^3 f_\gamma(x + c\rho \nabla f_\gamma(x)) (\nabla f_\gamma(x))^\alpha}{\alpha!} \right] \quad (27)$$

Now, we observe that

$$K_i(x) := \left[\sum_{|\alpha|=2} \frac{\partial_{e_i+\alpha}^3 f_\gamma(x + c\rho \nabla f_\gamma(x)) (\nabla f_\gamma(x))^\alpha}{\alpha!} \right] \quad (28)$$

is a finite sum of products of functions that by assumption are in G . Therefore, $K_i(x) \in G$ and $\bar{K}_i(x) = \mathbb{E}[K_i(x)] \in G$. Based on these definitions, we rewrite Eq. (27) as

$$\partial_{e_i} f_\gamma(x + \rho \nabla f_\gamma(x)) = \partial_{e_i} f_\gamma(x) + \rho \sum_j \partial_{e_i+e_j}^2 f_\gamma(x) \partial_{e_j} f_\gamma(x) + \rho^2 K_i(x). \quad (29)$$

which implies that

$$\mathbb{E}[\partial_{e_i} f_\gamma(x + \rho \nabla f_\gamma(x))] = \partial_{e_i} f(x) + \rho \mathbb{E} \left[\sum_j \partial_{e_i+e_j}^2 f_\gamma(x) \partial_{e_j} f_\gamma(x) \right] + \rho^2 \bar{K}_i(x). \quad (30)$$

Let us now remember that

$$\partial_{e_i} \tilde{f}^{\text{USAM}}(x) = \partial_{e_i} \left(f(x) + \frac{\rho}{2} \mathbb{E}[\|\nabla f_\gamma(x)\|_2^2] \right) = \partial_i f(x) + \rho \mathbb{E} \left[\sum_j \partial_{e_i+e_j}^2 f_\gamma(x) \partial_{e_j} f_\gamma(x) \right] \quad (31)$$

Therefore, by using Eq. (30), Eq. (31), and the assumption (24) we have that $\forall i = 1, \dots, d$

$$\mathbb{E} \bar{\Delta}_i = \partial_{e_i} \tilde{f}^{\text{USAM}}(x) \eta + \eta \rho^2 \bar{K}_i(x) = \partial_{e_i} \tilde{f}^{\text{USAM}}(x) \eta + \mathcal{O}(\eta^2). \quad (32)$$

Additionally, we have that

$$\begin{aligned} \mathbb{E} \bar{\Delta}_i \bar{\Delta}_j &= \text{Cov}(\bar{\Delta}_i, \bar{\Delta}_j) + \mathbb{E} \bar{\Delta}_i \mathbb{E} \bar{\Delta}_j \\ &\stackrel{(32)}{=} \text{Cov}(\bar{\Delta}_i, \bar{\Delta}_j) + \partial_i \tilde{f}^{\text{USAM}} \partial_j \tilde{f}^{\text{USAM}} \eta^2 + \eta^2 \rho^2 (\partial_i \tilde{f}^{\text{USAM}} \bar{K}_j(x) + \partial_j \tilde{f}^{\text{USAM}} \bar{K}_i(x)) + \eta^2 \rho^4 \bar{K}_i(x) \bar{K}_j(x) \\ &= \text{Cov}(\bar{\Delta}_i, \bar{\Delta}_j) + \partial_i \tilde{f}^{\text{USAM}} \partial_j \tilde{f}^{\text{USAM}} \eta^2 + \mathcal{O}(\eta^2 \rho^2) + \mathcal{O}(\eta^2 \rho^4) \\ &= \partial_i \tilde{f}^{\text{USAM}} \partial_j \tilde{f}^{\text{USAM}} \eta^2 + \text{Cov}(\bar{\Delta}_i, \bar{\Delta}_j) + \mathcal{O}(\eta^2 \rho^2) + \mathcal{O}(\eta^2 \rho^4) \quad \forall i, j = 1, \dots, d \end{aligned} \quad (33)$$

Let us now recall the expression (22) of Σ^* and the expression (23) of Σ^{USAM} . Then, we automatically have that

$$\text{Cov}(\bar{\Delta}_i, \bar{\Delta}_j) = \eta^2 (\Sigma_{i,j}^{\text{SGD}}(x) + \rho [\Sigma_{i,j}^*(x) + \Sigma_{i,j}^*(x)^\top] + \mathcal{O}(\rho^2)) = \eta^2 \Sigma_{i,j}^{\text{USAM}}(x) + \mathcal{O}(\eta^2 \rho^2) \quad (34)$$

Therefore, remembering Eq. (33) and Eq. (24) we have

$$\mathbb{E} \bar{\Delta}_i \bar{\Delta}_j = \partial_i \tilde{f}^{\text{USAM}} \partial_j \tilde{f}^{\text{USAM}} \eta^2 + \Sigma_{i,j}^{\text{SAM}} \eta^2 + \mathcal{O}(\eta^3), \quad \forall i, j = 1, \dots, d \quad (35)$$

Finally, with analogous considerations, it is obvious that under our assumptions

$$\mathbb{E} \prod_{j=1}^s \bar{\Delta}_{i_j} = \mathcal{O}(\eta^s) \quad \forall s \geq 3, \quad i_j \in \{1, \dots, d\}$$

which in particular implies that

$$\mathbb{E} \prod_{j=1}^3 \bar{\Delta}_{i_j} = \mathcal{O}(\eta^3), \quad i_j \in \{1, \dots, d\}.$$

□

Additional Insights from Lemma 12. Let us notice that $\nabla f_\gamma(x)$ is dominated by a factor $M(1+|x|)$, if all $\partial_{e_i+\alpha}^3 f_\gamma(x)$ are limited by a common constant L , for some positive constant C we have that

$$|K_i(x)| = \rho^2 \left| \sum_{|\alpha|=2} \frac{\partial_{e_i+\alpha}^3 f_\gamma(x + c\rho \nabla f_\gamma(x)) (\nabla f_\gamma(x))^\alpha}{\alpha!} \right| \quad (36)$$

$$\leq \rho^2 C L \|\nabla f_\gamma(x) \nabla f_\gamma(x)^\top\|_F^2 \leq \rho^2 C L d^2 M^2 (1+|x|)^2 \quad (37)$$

Therefore, $K_i(x)$ does not only lay in G , but has at most quadratic growth.

Proof of Theorem 11. To prove this result, all we need to do is check the conditions in Theorem 10. As we apply Lemma 9, we make the following choices:

- $b(x) = -\nabla \tilde{f}^{\text{USAM}}(x)$;
- $\sigma(x) = \Sigma^{\text{USAM}}(x)^{\frac{1}{2}}$.

First of all, we notice that $\forall i = 1, \dots, d$, it holds that

- $\mathbb{E} \bar{\Delta}_i \stackrel{1. \text{ Lemma } 12}{=} -\partial_i \tilde{f}^{\text{USAM}}(x) \eta + \mathcal{O}(\eta^2)$;
- $\mathbb{E} \Delta_i \stackrel{1. \text{ Lemma } 9}{=} -\partial_i \tilde{f}^{\text{USAM}}(x) \eta + \mathcal{O}(\eta^3)$.

Therefore, we have that for some $K_1(x) \in G$

$$|\mathbb{E} \Delta_i - \mathbb{E} \bar{\Delta}_i| \leq K_1(x) \eta^2, \quad \forall i = 1, \dots, d. \quad (38)$$

Additionally, we notice that $\forall i, j = 1 \dots d$, it holds that

- $\mathbb{E} \bar{\Delta}_i \bar{\Delta}_j \stackrel{2. \text{ Lemma } 12}{=} \partial_i \tilde{f}^{\text{USAM}} \partial_j \tilde{f}^{\text{USAM}} \eta^2 + \Sigma_{i,j}^{\text{USAM}} \eta^2 + \mathcal{O}(\eta^3)$;
- $\mathbb{E} \Delta_i \Delta_j \stackrel{2. \text{ Lemma } 9}{=} \partial_i \tilde{f}^{\text{USAM}} \partial_j \tilde{f}^{\text{USAM}} \eta^2 + \Sigma_{i,j}^{\text{USAM}} \eta^2 + \mathcal{O}(\eta^3)$.

Therefore, we have that for some $K_2(x) \in G$

$$|\mathbb{E} \Delta_i \Delta_j - \mathbb{E} \bar{\Delta}_i \bar{\Delta}_j| \leq K_2(x) \eta^2, \quad \forall i, j = 1 \dots d \quad (39)$$

Additionally, we notice that $\forall s \geq 3, \forall i_j \in \{1 \dots d\}$, it holds that

- $\mathbb{E} \prod_{j=1}^s \bar{\Delta}_{i_j} \stackrel{3. \text{ Lemma } 12}{=} \mathcal{O}(\eta^3)$;
- $\mathbb{E} \prod_{j=1}^s \Delta_{i_j} \stackrel{3. \text{ Lemma } 9}{=} \mathcal{O}(\eta^3)$.

Therefore, we have that for some $K_3(x) \in G$

$$\left| \mathbb{E} \prod_{j=1}^s \Delta_{i_j} - \mathbb{E} \prod_{j=1}^s \bar{\Delta}_{i_j} \right| \leq K_3(x) \eta^2. \quad (40)$$

Additionally, for some $K_4(x) \in G, \forall i_j \in \{1 \dots d\}$

$$\mathbb{E} \prod_{j=1}^3 |\bar{\Delta}_{(i_j)}| \stackrel{3. \text{ Lemma } 12}{\leq} K_4(x) \eta^2. \quad (41)$$

Finally, Eq. (38), Eq. (39), Eq. (40), and Eq. (41) allow us to conclude the proof. \square

Corollary 13. *Let us take the same assumptions of Theorem 11. Additionally, let us assume that the dynamics is near the minimizer. In this case, the noise structure is such that the stochastic gradient can be written as $\nabla f_\gamma(x) = \nabla f(x) + Z$ such that Z is the noise that does not depend on x . Therefore, the SDE (21) becomes*

$$dX_t = -\nabla \tilde{f}^{\text{USAM}}(X_t)dt + (Id + \rho \nabla^2 f(X_t)) (\eta \Sigma^{\text{SGD}}(X_t))^{\frac{1}{2}} dW_t \quad (42)$$

where

$$\Sigma^{\text{SGD}}(x) := \mathbb{E} \left[(\nabla f(x) - \nabla f_\gamma(x)) (\nabla f(x) - \nabla f_\gamma(x))^T \right]$$

is the usual covariance of SGD, and

$$\tilde{f}^{\text{USAM}}(x) = \frac{\rho}{2} \|\nabla f(x)\|_2^2.$$

Proof of Corollary 13. Based on our assumption on the noise structure, we can rewrite Eq. (22) of the matrix Σ^* as

$$\Sigma^*(x) = \mathbb{E} \left[(\nabla f(x) - \nabla f_\gamma(x)) (\mathbb{E} [\nabla^2 f_\gamma(x) \nabla f_\gamma(x)] - \nabla^2 f_\gamma(x) \nabla f_\gamma(x))^T \right] \quad (43)$$

$$= \nabla^2 f(x) \mathbb{E} \left[(\nabla f(x) - \nabla f_\gamma(x)) (\nabla f(x) - \nabla f_\gamma(x))^T \right] \quad (44)$$

Therefore, the Eq. (23) of the covariance Σ^{USAM} becomes

$$\Sigma^{\text{USAM}}(x) = (Id + 2\rho \nabla^2 f(x)) \Sigma^{\text{SGD}}(X_t) \quad (45)$$

which implies that

$$(\Sigma^{\text{USAM}}(x))^{\frac{1}{2}} \approx (Id + \rho \nabla^2 f(x)) (\Sigma^{\text{SGD}}(X_t))^{\frac{1}{2}}. \quad (46)$$

Finally, we have that

$$\tilde{f}^{\text{USAM}}(x) := f(x) + \frac{\rho}{2} \mathbb{E} [\|\nabla f_\gamma(x)\|_2^2] = f(x) + \frac{\rho}{2} \mathbb{E} [\|\nabla f(x)\|_2^2 + Z^2 + 2Z \nabla f_\gamma(x)] \quad (47)$$

$$= f(x) + \frac{\rho}{2} \|\nabla f(x)\|_2^2 + \frac{\rho}{2} \mathbb{E} [Z^2] \quad (48)$$

Since the component $\mathbb{E} [Z^2]$ is independent on x , we ignore it and conclude that

$$\tilde{f}^{\text{USAM}}(x) = \frac{\rho}{2} \|\nabla f(x)\|_2^2.$$

□

A.1.1 USAM is SGD if $\rho = \mathcal{O}(\eta)$

The following result is inspired by Theorem 1 of Li et al. (2017).

Theorem 14 (Stochastic modified equations). *Let $0 < \eta < 1, T > 0$ and set $N = \lfloor T/\eta \rfloor$. Let $x_k \in \mathbb{R}^d, 0 \leq k \leq N$ denote a sequence of USAM iterations defined by Eq. (5). Additionally, let us take*

$$\rho = \mathcal{O}(\eta^1). \quad (49)$$

Define $X_t \in \mathbb{R}^d$ as the stochastic process satisfying the SDE

$$dX_t = -\nabla f(X_t) dt + (\eta \Sigma^{SGD}(X_t))^{1/2} dW_t \quad (50)$$

Such that $X_0 = x_0$ and

$$\Sigma^{SGD}(x) := \mathbb{E} \left[(\nabla f(x) - \nabla f_\gamma(x)) (\nabla f(x) - \nabla f_\gamma(x))^T \right]$$

Fix some test function $g \in G$ and suppose that g and its partial derivatives up to order 6 belong to G .

Then, under Assumption 1, there exists a constant $C > 0$ independent of η such that for all $k = 0, 1, \dots, N$, we have

$$|\mathbb{E}g(X_{k\eta}) - \mathbb{E}g(x_k)| \leq C\eta^1.$$

That is, the SDE (50) is an order 1 weak approximation of the USAM iterations (5).

Lemma 15. *Under the assumptions of Theorem 14, let $0 < \eta < 1$. Consider $x_k, k \geq 0$ satisfying the USAM iterations*

$$x_{k+1} = x_k - \eta \nabla f_{\gamma_k}(x_k + \rho \nabla f_{\gamma_k}(x_k))$$

with $x_0 = x \in \mathbb{R}^d$. From the definition the one-step difference $\bar{\Delta} = x_1 - x$, then we have

1. $\mathbb{E}\bar{\Delta}_i = -\partial_i f(x)\eta + \mathcal{O}(\eta^2) \quad \forall i = 1, \dots, d$.
2. $\mathbb{E}\bar{\Delta}_i \bar{\Delta}_j = \partial_i f \partial_j f \eta^2 + \Sigma_{(ij)}^{SGD} \eta^2 + \mathcal{O}(\eta^3) \quad \forall i, j = 1, \dots, d$.
3. $\mathbb{E} \prod_{j=1}^s \bar{\Delta}_{i_j} = \mathcal{O}(\eta^3) \quad \forall s \geq 3, \quad i_j \in \{1, \dots, d\}$.

All functions above are evaluated at x .

Proof of Lemma 15. First of all, we write that

$$\partial_{e_i} f_\gamma(x + \rho \nabla f_\gamma(x)) = \partial_{e_i} f_\gamma(x) + \mathcal{R}_{x,0}^{\partial_{e_i} f_\gamma(x)}(\rho \nabla f_\gamma(x)), \quad (51)$$

where the residual is defined in Eq. (4) of Folland (2005). Therefore, for some constant $c \in (0, 1)$, it holds that

$$\mathcal{R}_{x,0}^{\partial_{e_i} f_\gamma(x)}(\rho \nabla f_\gamma(x)) = \sum_{|\alpha|=1} \frac{\partial_{e_i + \alpha}^2 f_\gamma(x + c\rho \nabla f_\gamma(x)) \rho^1 (\nabla f_\gamma(x))^\alpha}{\alpha!}. \quad (52)$$

Let us now observe that $\mathcal{R}_{x,0}^{\partial_{e_i} f_\gamma(x)}(\rho \nabla f_\gamma(x))$ is a finite sum of products of functions in G and that, therefore, it lies in G . Additionally, given its expression Eq. (52), we can factor out a common ρ and have that $K(x) = \rho K_1(x)$ for some function $K_1(x) \in G$. Therefore, we rewrite Eq. (51) as

$$\partial_{e_i} f_\gamma(x + \rho \nabla f_\gamma(x)) = \partial_{e_i} f_\gamma(x) + \rho K_1(x). \quad (53)$$

First of all, we notice that if we define $\bar{K}_1(x) = \mathbb{E}[K_1(x)]$, also $\bar{K}_1(x) \in G$. Therefore, it holds that

$$\mathbb{E}[\partial_{e_i} f_\gamma(x + \rho \nabla f_\gamma(x))] \stackrel{(53)}{=} \partial_{e_i} f(x) + \rho \bar{K}_1(x) \quad (54)$$

Therefore, using assumption (49), $\forall i = 1, \dots, d$, we have that

$$\mathbb{E} \bar{\Delta}_i = -\partial_i f(x) \eta + \eta \rho \bar{K}_i(x) = \partial_{e_i} f(x) \eta + \mathcal{O}(\eta^2) \quad (55)$$

Additionally, by keeping in mind the definition of the covariance matrix Σ , We immediately have

$$\begin{aligned} \mathbb{E} \bar{\Delta}_i \bar{\Delta}_j &\stackrel{(53)}{=} \text{Cov}(\bar{\Delta}_i, \bar{\Delta}_j) + \mathbb{E} \bar{\Delta}_i \mathbb{E} \bar{\Delta}_j \\ &= \Sigma_{(ij)}^{\text{SGD}} \eta^2 + \partial_i f \partial_j f \eta^2 + \eta^2 \rho (\partial_i f \bar{K}_j(x) + \partial_j f \bar{K}_i(x)) + \eta^2 \rho^2 \bar{K}_i(x) \bar{K}_j(x) \\ &= \Sigma_{(ij)}^{\text{SGD}} \eta^2 + \partial_i f \partial_j f \eta^2 + \mathcal{O}(\eta^2 \rho) + \mathcal{O}(\eta^2 \rho^2) \\ &= \partial_i f \partial_j f \eta^2 + \Sigma_{(ij)}^{\text{SGD}} \eta^2 + \mathcal{O}(\eta^3) \quad \forall i, j = 1, \dots, d \end{aligned} \quad (56)$$

Finally, with analogous considerations, it is obvious that under our assumptions

$$\mathbb{E} \prod_{j=1}^s \bar{\Delta}_{i_j} = \mathcal{O}(\eta^3) \quad \forall s \geq 3, \quad i_j \in \{1, \dots, d\}.$$

□

Proof of Theorem 14. To prove this result, all we need to do is check the conditions in Theorem 10. As we apply Lemma 9, we make the following choices:

- $b(x) = -\nabla f(x)$,
- $\sigma(x) = \Sigma^{\text{SGD}}(X_t)^{\frac{1}{2}}$;

First of all, we notice that $\forall i = 1, \dots, d$, it holds that

- $\mathbb{E} \bar{\Delta}_i \stackrel{1. \text{ Lemma } 15}{=} -\partial_i f(x) \eta + \mathcal{O}(\eta^2)$;
- $\mathbb{E} \Delta_i \stackrel{1. \text{ Lemma } 9}{=} -\partial_i f(x) \eta + \mathcal{O}(\eta^2)$.

Therefore, we have that for some $K_1(x) \in G$

$$|\mathbb{E} \Delta_i - \mathbb{E} \bar{\Delta}_i| \leq K_1(x) \eta^2, \quad \forall i = 1, \dots, d. \quad (57)$$

Additionally, we notice that $\forall i, j = 1, \dots, d$, it holds that

- $\mathbb{E} \bar{\Delta}_i \bar{\Delta}_j \stackrel{2. \text{ Lemma } 15}{=} \partial_i f \partial_j f \eta^2 + \Sigma_{(ij)}^{\text{SGD}} \eta^2 + \mathcal{O}(\eta^3)$;
- $\mathbb{E} \Delta_i \Delta_j \stackrel{2. \text{ Lemma } 9}{=} \partial_i f \partial_j f \eta^2 + \Sigma_{(ij)}^{\text{SGD}} \eta^2 + \mathcal{O}(\eta^3)$.

Therefore, we have that for some $K_2(x) \in G$

$$|\mathbb{E} \Delta_i \Delta_j - \mathbb{E} \bar{\Delta}_i \bar{\Delta}_j| \leq K_2(x) \eta^2, \quad \forall i, j = 1, \dots, d \quad (58)$$

Additionally, we notice that $\forall s \geq 3, \forall i_j \in \{1, \dots, d\}$, it holds that

- $\mathbb{E} \prod_{j=1}^s \bar{\Delta}_{i_j} \stackrel{3. \text{ Lemma } 15}{=} \mathcal{O}(\eta^3)$;

- $\mathbb{E} \prod_{j=1}^s \Delta_{i_j} \stackrel{3. \text{ Lemma 9}}{=} \mathcal{O}(\eta^3)$.

Therefore, we have that for some $K_3(x) \in G$

$$\left| \mathbb{E} \prod_{j=1}^s \Delta_{i_j} - \mathbb{E} \prod_{j=1}^s \bar{\Delta}_{i_j} \right| \leq K_3(x) \eta^2. \quad (59)$$

Additionally, for some $K_4(x) \in G$, $\forall i_j \in \{1 \dots d\}$

$$\mathbb{E} \prod_{j=1}^3 |\bar{\Delta}_{(i_j)}| \stackrel{3. \text{ Lemma 15}}{\leq} K_4(x) \eta^2. \quad (60)$$

Finally, Eq. (57), Eq. (58), Eq. (59), and Eq. (60) allow us to conclude the proof. \square

A.2 Formal Derivation - SAM

The following result is inspired by Theorem 1 of Li et al. (2017). We will consider the stochastic process $X_t \in \mathbb{R}^d$ defined as the solution of the SDE

$$dX_t = -\nabla \tilde{f}^{\text{SAM}}(X_t) dt + \sqrt{\eta} (\Sigma^{\text{SGD}}(X_t) + \rho (\Sigma^{**}(X_t) + \Sigma^{**}(X_t)^\top))^{\frac{1}{2}} dW_t \quad (61)$$

where

$$\Sigma^{\text{SGD}}(x) := \mathbb{E} \left[(\nabla f(x) - \nabla f_\gamma(x)) (\nabla f(x) - \nabla f_\gamma(x))^T \right]$$

is the usual covariance of SGD, while

$$\Sigma^{**}(x) := \mathbb{E} \left[(\nabla f(x) - \nabla f_\gamma(x)) \left(\mathbb{E} \left[\frac{\nabla^2 f_\gamma(x) \nabla f_\gamma(x)}{\|\nabla f_\gamma(x)\|_2} \right] - \frac{\nabla^2 f_\gamma(x) \nabla f_\gamma(x)}{\|\nabla f_\gamma(x)\|_2} \right)^\top \right] \quad (62)$$

and

$$\tilde{f}^{\text{SAM}}(x) := f(x) + \rho \mathbb{E} [\|\nabla f_\gamma(x)\|_2].$$

In the following, we will use the notation

$$\Sigma^{\text{SAM}}(x) := (\Sigma^{\text{SGD}}(X_t) + \rho (\Sigma^{**}(X_t) + \Sigma^{**}(X_t)^\top)). \quad (63)$$

Theorem 16 (Stochastic modified equations). *Let $0 < \eta < 1, T > 0$ and set $N = \lfloor T/\eta \rfloor$. Let $x_k \in \mathbb{R}^d, 0 \leq k \leq N$ denote a sequence of SAM iterations defined by Eq. (4). Additionally, let us take*

$$\rho = \mathcal{O}(\eta^{\frac{1}{2}}). \quad (64)$$

Consider the stochastic process X_t defined in Eq. (61) and fix some test function $g \in G$ and suppose that g and its partial derivatives up to order 6 belong to G .

Then, under Assumption 1, there exists a constant $C > 0$ independent of η such that for all $k = 0, 1, \dots, N$, we have

$$|\mathbb{E}g(X_{k\eta}) - \mathbb{E}g(x_k)| \leq C\eta^1.$$

That is, the SDE (61) is an order 1 weak approximation of the SAM iterations (4).

Lemma 17. Under the assumptions of Theorem 16, let $0 < \eta < 1$ and consider $x_k, k \geq 0$ satisfying the USA iterations (4)

$$x_{k+1} = x_k - \eta \nabla f_{\gamma_k} \left(x_k + \rho \frac{\nabla f_{\gamma_k}(x_k)}{\|\nabla f_{\gamma_k}(x_k)\|} \right)$$

with $x_0 = x \in \mathbb{R}^d$. Additionally, we define $\partial_i \tilde{f}^{SAM}(x) := \partial_{e_i} f(x) + \rho \mathbb{E} \left[\frac{\sum_j \partial_{e_i+e_j}^2 f_{\gamma}(x) \partial_{e_j} f_{\gamma}(x)}{\|\nabla f_{\gamma}(x)\|} \right]$. From the definition the one-step difference $\bar{\Delta} = x_1 - x$, then we have

1. $\mathbb{E} \bar{\Delta}_i = -\partial_i \tilde{f}^{SAM}(x) \eta + \mathcal{O}(\eta \rho^2) \quad \forall i = 1, \dots, d;$
2. $\mathbb{E} \bar{\Delta}_i \bar{\Delta}_j = \partial_i \tilde{f}^{SAM}(x) \partial_j \tilde{f}^{SAM}(x) \eta^2 + \Sigma_{(ij)}^{SAM} \eta^2 + \mathcal{O}(\eta^3) \quad \forall i, j = 1, \dots, d;$
3. $\mathbb{E} \prod_{j=1}^s \Delta_{i_j} = \mathcal{O}(\eta^3) \quad \forall s \geq 3, \quad i_j \in \{1, \dots, d\}.$

and all the functions above are evaluated at x .

Proof of Lemma 17. Since the first step is to evaluate $\mathbb{E} \Delta_i = \mathbb{E} \left[\partial_{e_i} f_{\gamma} \left(x + \frac{\rho}{\|\nabla f_{\gamma}(x)\|} \nabla f_{\gamma}(x) \right) \eta \right]$, we start by analyzing $\partial_{e_i} f_{\gamma} \left(x + \frac{\rho}{\|\nabla f_{\gamma}(x)\|} \nabla f_{\gamma}(x) \right)$, that is the partial derivative in the direction $e_i := (0, \dots, 0, \underset{i-th}{1}, 0, \dots, 0)$. Then, we have that

$$\partial_{e_i} f_{\gamma} \left(x + \frac{\rho}{\|\nabla f_{\gamma}(x)\|} \nabla f_{\gamma}(x) \right) = \partial_{e_i} f_{\gamma}(x) + \sum_{|\alpha|=1} \partial_{e_i+\alpha}^2 f_{\gamma}(x) \rho \frac{\partial_{\alpha} f_{\gamma}(x)}{\|\nabla f_{\gamma}(x)\|} + \mathcal{R}_{x,1}^{\partial_{e_i} f_{\gamma}(x)} \left(\rho \frac{\nabla f_{\gamma}(x)}{\|\nabla f_{\gamma}(x)\|} \right) \quad (65)$$

Where the residual is defined in Eq. (4) of Folland (2005). Therefore, for some constant $c \in (0, 1)$, it holds that

$$\mathcal{R}_{x,1}^{\partial_{e_i} f_{\gamma}(x)} \left(\rho \frac{\nabla f_{\gamma}(x)}{\|\nabla f_{\gamma}(x)\|} \right) = \sum_{|\alpha|=2} \frac{\partial_{e_i+\alpha}^3 f_{\gamma} \left(x + c\rho \frac{\nabla f_{\gamma}(x)}{\|\nabla f_{\gamma}(x)\|} \right) \rho^2 \left(\frac{\nabla f_{\gamma}(x)}{\|\nabla f_{\gamma}(x)\|} \right)^{\alpha}}{\alpha!}. \quad (66)$$

Therefore, we can rewrite it as

$$\partial_{e_i} f_{\gamma} \left(x + \frac{\rho}{\|\nabla f_{\gamma}(x)\|} \nabla f_{\gamma}(x) \right) = \partial_{e_i} f_{\gamma}(x) + \frac{\rho}{\|\nabla f_{\gamma}(x)\|} \sum_{|\alpha|=1} \partial_{e_i+\alpha}^2 f_{\gamma}(x) \partial_{\alpha} f_{\gamma}(x) \quad (67)$$

$$+ \rho^2 \sum_{|\alpha|=2} \frac{\partial_{e_i+\alpha}^3 f_{\gamma} \left(x + c\rho \frac{\nabla f_{\gamma}(x)}{\|\nabla f_{\gamma}(x)\|} \right) \left(\frac{\nabla f_{\gamma}(x)}{\|\nabla f_{\gamma}(x)\|} \right)^{\alpha}}{\alpha!}. \quad (68)$$

Now, we observe that

$$K_i(x) := \left[\sum_{|\alpha|=2} \frac{\partial_{e_i+\alpha}^3 f_{\gamma} \left(x + c\rho \frac{\nabla f_{\gamma}(x)}{\|\nabla f_{\gamma}(x)\|} \right) \left(\frac{\nabla f_{\gamma}(x)}{\|\nabla f_{\gamma}(x)\|} \right)^{\alpha}}{\alpha!} \right] \quad (69)$$

is a finite sum of products of functions that by assumption are in G . Therefore, $K_i(x) \in G$ and $\bar{K}_i(x) = \mathbb{E}[K_i(x)] \in G$. Based on these definitions, we rewrite Eq. (67) as

$$\partial_{e_i} f_{\gamma} \left(x + \frac{\rho}{\|\nabla f_{\gamma}(x)\|} \nabla f_{\gamma}(x) \right) = \partial_{e_i} f_{\gamma}(x) + \frac{\rho}{\|\nabla f_{\gamma}(x)\|} \sum_{|\alpha|=1} \partial_{e_i+\alpha}^2 f_{\gamma}(x) \partial_{\alpha} f_{\gamma}(x) + \rho^2 K_i(x). \quad (70)$$

which implies that

$$\mathbb{E} \left[\partial_{e_i} f_\gamma \left(x + \frac{\rho}{\|\nabla f_\gamma(x)\|} \nabla f_\gamma(x) \right) \right] = \partial_{e_i} f(x) + \rho \mathbb{E} \left[\frac{\sum_j \partial_{e_i+e_j}^2 f_\gamma(x) \partial_{e_j} f_\gamma(x)}{\|\nabla f_\gamma(x)\|} \right] + \rho^2 \bar{K}_i(x). \quad (71)$$

Let us now remember that

$$\partial_{e_i} \tilde{f}^{\text{SAM}}(x) = \partial_{e_i} (f(x) + \rho \mathbb{E} [\|\nabla f_\gamma(x)\|_2]) = \partial_{e_i} f(x) + \rho \mathbb{E} \left[\frac{\sum_j \partial_{e_i+e_j}^2 f_\gamma(x) \partial_{e_j} f_\gamma(x)}{\|\nabla f_\gamma(x)\|} \right] \quad (72)$$

Therefore, by using Eq. (71), Eq. (72), and the assumption (64) we have that $\forall i = 1, \dots, d$

$$\mathbb{E} \bar{\Delta}_i = \partial_{e_i} \tilde{f}^{\text{SAM}}(x) \eta + \eta \rho^2 \bar{K}_i(x) = \partial_{e_i} \tilde{f}^{\text{SAM}}(x) \eta + \mathcal{O}(\eta^2). \quad (73)$$

Additionally, we have that

$$\begin{aligned} \mathbb{E} \bar{\Delta}_i \bar{\Delta}_j &= \text{Cov}(\bar{\Delta}_i, \bar{\Delta}_j) + \mathbb{E} \bar{\Delta}_i \mathbb{E} \bar{\Delta}_j \\ &\stackrel{(73)}{=} \text{Cov}(\bar{\Delta}_i, \bar{\Delta}_j) + \partial_i \tilde{f}^{\text{SAM}} \partial_j \tilde{f}^{\text{SAM}} \eta^2 + \eta^2 \rho^2 (\partial_i \tilde{f}^{\text{SAM}} \bar{K}_j(x) + \partial_j \tilde{f}^{\text{SAM}} \bar{K}_i(x)) + \eta^2 \rho^4 \bar{K}_i(x) \bar{K}_j(x) \\ &= \text{Cov}(\bar{\Delta}_i, \bar{\Delta}_j) + \partial_i \tilde{f}^{\text{SAM}} \partial_j \tilde{f}^{\text{SAM}} \eta^2 + \mathcal{O}(\eta^2 \rho^2) + \mathcal{O}(\eta^2 \rho^4) \\ &= \partial_i \tilde{f}^{\text{SAM}} \partial_j \tilde{f}^{\text{SAM}} \eta^2 + \text{Cov}(\bar{\Delta}_i, \bar{\Delta}_j) + \mathcal{O}(\eta^2 \rho^2) + \mathcal{O}(\eta^2 \rho^4) \quad \forall i, j = 1, \dots, d. \end{aligned} \quad (74)$$

Let us now recall the expression (62) of Σ^{**} and the expression (63) of Σ^{SAM} . Then, we automatically have that

$$\text{Cov}(\bar{\Delta}_i, \bar{\Delta}_j) = \eta^2 (\Sigma_{i,j}^{\text{SGD}}(x) + \rho [\Sigma_{i,j}^{**}(x) + \Sigma_{i,j}^{**}(x)^\top] + \mathcal{O}(\rho^2)) = \eta^2 \Sigma_{i,j}^{\text{SAM}}(x) + \mathcal{O}(\eta^2 \rho^2). \quad (75)$$

Therefore, remembering Eq. (74) and Eq. (64) we have

$$\mathbb{E} \bar{\Delta}_i \bar{\Delta}_j = \partial_i \tilde{f}^{\text{SAM}} \partial_j \tilde{f}^{\text{SAM}} \eta^2 + \Sigma_{i,j}^{\text{SAM}} \eta^2 + \mathcal{O}(\eta^3), \quad \forall i, j = 1, \dots, d. \quad (76)$$

Finally, with analogous considerations, it is obvious that under our assumptions

$$\mathbb{E} \prod_{j=1}^s \bar{\Delta}_{i_j} = \mathcal{O}(\eta^s) \quad \forall s \geq 3, \quad i_j \in \{1, \dots, d\}$$

which in particular implies that

$$\mathbb{E} \prod_{j=1}^3 \bar{\Delta}_{i_j} = \mathcal{O}(\eta^3), \quad i_j \in \{1, \dots, d\}.$$

□

Proof of Theorem 16. To prove this result, all we need to do is check the conditions in Theorem 10. As we apply Lemma 9, we make the following choices:

- $b(x) = -\nabla \tilde{f}^{\text{SAM}}(x)$;
- $\sigma(x) = \Sigma^{\text{SAM}}(x)^{\frac{1}{2}}$.

First of all, we notice that $\forall i = 1, \dots, d$, it holds that

- $\mathbb{E} \bar{\Delta}_i \stackrel{1. \text{ Lemma 17}}{=} -\partial_i \tilde{f}^{\text{SAM}}(x) \eta + \mathcal{O}(\eta^2)$;

- $\mathbb{E}\Delta_i \stackrel{1. \text{ Lemma } 9}{=} -\partial_i \tilde{f}^{\text{SAM}}(x)\eta + \mathcal{O}(\eta^3).$

Therefore, we have that for some $K_1(x) \in G$

$$|\mathbb{E}\Delta_i - \mathbb{E}\bar{\Delta}_i| \leq K_1(x)\eta^2, \quad \forall i = 1, \dots, d. \quad (77)$$

Additionally, we notice that $\forall i, j = 1 \dots d$, it holds that

- $\mathbb{E}\bar{\Delta}_i \bar{\Delta}_j \stackrel{2. \text{ Lemma } 17}{=} \partial_i \tilde{f}^{\text{SAM}} \partial_j \tilde{f}^{\text{SAM}} \eta^2 + \Sigma_{i,j}^{\text{SAM}} \eta^2 + \mathcal{O}(\eta^3);$
- $\mathbb{E}\Delta_i \Delta_j \stackrel{2. \text{ Lemma } 9}{=} \partial_i \tilde{f}^{\text{SAM}} \partial_j \tilde{f}^{\text{SAM}} \eta^2 + \Sigma_{i,j}^{\text{SAM}} \eta^2 + \mathcal{O}(\eta^3).$

Therefore, we have that for some $K_2(x) \in G$

$$|\mathbb{E}\Delta_i \Delta_j - \mathbb{E}\bar{\Delta}_i \bar{\Delta}_j| \leq K_2(x)\eta^2, \quad \forall i, j = 1 \dots d. \quad (78)$$

Additionally, we notice that $\forall s \geq 3, \forall i_j \in \{1 \dots d\}$, it holds that

- $\mathbb{E}\prod_{j=1}^s \bar{\Delta}_{i_j} \stackrel{3. \text{ Lemma } 17}{=} \mathcal{O}(\eta^3);$
- $\mathbb{E}\prod_{j=1}^s \Delta_{i_j} \stackrel{3. \text{ Lemma } 9}{=} \mathcal{O}(\eta^3).$

Therefore, we have that for some $K_3(x) \in G$

$$\left| \mathbb{E}\prod_{j=1}^s \Delta_{i_j} - \mathbb{E}\prod_{j=1}^s \bar{\Delta}_{i_j} \right| \leq K_3(x)\eta^2. \quad (79)$$

Additionally, for some $K_4(x) \in G, \forall i_j \in \{1 \dots d\}$

$$\mathbb{E}\prod_{j=1}^3 |\bar{\Delta}_{(i_j)}| \stackrel{3. \text{ Lemma } 12}{\leq} K_4(x)\eta^2. \quad (80)$$

Finally, Eq. (77), Eq. (78), Eq. (79), and Eq. (80) allow us to conclude the proof. □

Corollary 18. *Let us take the same assumptions of Theorem (16). Additionally, let us assume that the dynamics is near the minimizer. In this case, the noise structure is such that the stochastic gradient can be written as $\nabla f_\gamma(x) = \nabla f(x) + Z$ such that Z is the noise that does not depend on x . Additionally, we consider the iteration:*

$$x_{k+1} = x_k - \eta \nabla f_{\gamma_k} \left(x_k + \rho \frac{\nabla f_{\gamma_k}(x_k)}{\|\nabla f(x_k)\|} \right). \quad (81)$$

In this case, the SDE (61) becomes

$$dX_t = -\nabla \tilde{f}^{\text{SAM}}(X_t)dt + \left(Id + \rho \frac{\nabla^2 f(X_t)}{\|\nabla f(X_t)\|_2} \right) \left(\eta \Sigma^{\text{SGD}}(X_t) \right)^{\frac{1}{2}} dW_t \quad (82)$$

where

$$\Sigma^{\text{SGD}}(x) := \mathbb{E} \left[(\nabla f(x) - \nabla f_\gamma(x)) (\nabla f(x) - \nabla f_\gamma(x))^T \right]$$

is the usual covariance of SGD, and

$$\tilde{f}^{\text{SAM}}(x) = f(x) + \rho \|\nabla f(x)\|_2.$$

Proof of Corollary 18. Based on our assumption on the noise structure, we can rewrite Eq. (62) of the matrix Σ^{**} as

$$\Sigma^{**}(x) := \mathbb{E} \left[(\nabla f(x) - \nabla f_\gamma(x)) \left(\mathbb{E} \left[\frac{\nabla^2 f_\gamma(x) \nabla f_\gamma(x)}{\|\nabla f(x)\|_2} \right] - \frac{\nabla^2 f_\gamma(x) \nabla f_\gamma(x)}{\|\nabla f(x)\|_2} \right)^\top \right] \quad (83)$$

$$= \frac{\nabla^2 f(x)}{\|\nabla f(x)\|_2} \mathbb{E} \left[(\nabla f(x) - \nabla f_\gamma(x)) (\nabla f(x) - \nabla f_\gamma(x))^\top \right]. \quad (84)$$

Therefore, the Eq. (63) of the covariance Σ^{SAM} becomes

$$\Sigma^{\text{SAM}}(x) = \left(Id + 2\rho \frac{\nabla^2 f(x)}{\|\nabla f(x)\|_2} \right) \Sigma^{\text{SGD}}(X_t) \quad (85)$$

which implies that

$$(\Sigma^{\text{USAM}}(x))^{\frac{1}{2}} \approx \left(Id + \rho \frac{\nabla^2 f(x)}{\|\nabla f(x)\|_2} \right) (\Sigma^{\text{SGD}}(X_t))^{\frac{1}{2}}. \quad (86)$$

Finally, we have that

$$f(x) + \rho \|\nabla f(x)\|_2 \leq \tilde{f}^{\text{SAM}}(x) := f(x) + \rho \mathbb{E} [\|\nabla f_\gamma(x)\|_2] \leq f(x) + \rho \|\nabla f(x)\|_2 + \text{std}(Z). \quad (87)$$

Given these inequalities, we argue that in this case

$$\tilde{f}^{\text{SAM}}(x) = f(x) + \rho \|\nabla f(x)\|_2.$$

□

A.2.1 SAM is SGD if $\rho = \mathcal{O}(\eta)$

The following result is inspired by Theorem 1 of Li et al. (2017). We will consider the stochastic process $X_t \in \mathbb{R}^d$ defined as the solution of the SDE

$$dX_t = -\nabla f(X_t) dt + (\eta \Sigma^{\text{SGD}}(X_t))^{1/2} dW_t \quad (88)$$

Such that $X_0 = x_0$ and

$$\Sigma^{\text{SGD}}(x) := \mathbb{E} \left[(\nabla f(x) - \nabla f_\gamma(x)) (\nabla f(x) - \nabla f_\gamma(x))^\top \right]$$

Theorem 19 (Stochastic modified equations). *Let $0 < \eta < 1, T > 0$ and set $N = \lfloor T/\eta \rfloor$. Let $x_k \in \mathbb{R}^d, 0 \leq k \leq N$ denote a sequence of SAM iterations defined by Eq. (4). Additionally, let us take*

$$\rho = \mathcal{O}(\eta^1). \quad (89)$$

Consider the stochastic process X_t defined in Eq. (88) and fix some test function $g \in G$ and suppose that g and its partial derivatives up to order 6 belong to G . Then, under Assumption 1, there exists a constant $C > 0$ independent of η such that for all $k = 0, 1, \dots, N$, we have

$$|\mathbb{E}g(X_{k\eta}) - \mathbb{E}g(x_k)| \leq C\eta^1.$$

That is, the SDE (88) is an order 1 weak approximation of the SAM iterations (4).

Lemma 20. Under the assumptions of Theorem 19, let $0 < \eta < 1$. Consider $x_k, k \geq 0$ satisfying the SAM iterations

$$x_{k+1} = x_k - \eta \nabla f_{\gamma_k} \left(x_k + \rho \frac{\nabla f_{\gamma_k}(x_k)}{\|\nabla f_{\gamma_k}(x_k)\|} \right)$$

with $x_0 = x \in \mathbb{R}^d$. From the definition the one-step difference $\bar{\Delta} = x_1 - x$, then we have

1. $\mathbb{E} \bar{\Delta}_i = -\partial_i f(x) \eta + \mathcal{O}(\eta^2) \quad \forall i = 1, \dots, d$.
2. $\mathbb{E} \bar{\Delta}_i \bar{\Delta}_j = \partial_i f \partial_j f \eta^2 + \Sigma_{(ij)}^{SGD} \eta^2 + \mathcal{O}(\eta^3) \quad \forall i, j = 1, \dots, d$.
3. $\mathbb{E} \prod_{j=1}^s \bar{\Delta}_{i_j} = \mathcal{O}(\eta^3) \quad \forall s \geq 3, \quad i_j \in \{1, \dots, d\}$.

All functions above are evaluated at x .

Proof of Lemma 20. First of all, we write that

$$\partial_{e_i} f_\gamma \left(x + \rho \frac{\nabla f_\gamma(x)}{\|\nabla f_\gamma(x)\|} \right) = \partial_{e_i} f_\gamma(x) + \mathcal{R}_{x,0}^{\partial_{e_i} f_\gamma(x)} \left(\rho \frac{\nabla f_\gamma(x)}{\|\nabla f_\gamma(x)\|} \right), \quad (90)$$

where the residual is defined in Eq. (4) of Folland (2005). Therefore, for some constant $c \in (0, 1)$, it holds that

$$\mathcal{R}_{x,0}^{\partial_{e_i} f_\gamma(x)} \left(\rho \frac{\nabla f_\gamma(x)}{\|\nabla f_\gamma(x)\|} \right) = \sum_{|\alpha|=1} \frac{\partial_{e_i+\alpha}^2 f_\gamma \left(x + c \rho \frac{\nabla f_\gamma(x)}{\|\nabla f_\gamma(x)\|} \right) \rho^1 \left(\frac{\nabla f_\gamma(x)}{\|\nabla f_\gamma(x)\|} \right)^\alpha}{\alpha!}. \quad (91)$$

Let us now observe that $\mathcal{R}_{x,0}^{\partial_{e_i} f_\gamma(x)} \left(\rho \frac{\nabla f_\gamma(x)}{\|\nabla f_\gamma(x)\|} \right)$ is a finite sum of products of functions in G and that, therefore, it lies in G . Additionally, given its expression Eq. (91), we can factor out a common ρ and have that $K(x) = \rho K_1(x)$ for some function $K_1(x) \in G$. Therefore, we rewrite Eq. (90) as

$$\partial_{e_i} f_\gamma \left(x + \rho \frac{\nabla f_\gamma(x)}{\|\nabla f_\gamma(x)\|} \right) = \partial_{e_i} f_\gamma(x) + \rho K_1(x). \quad (92)$$

First of all, we notice that if we define $\bar{K}_1(x) = \mathbb{E}[K_1(x)]$, also $\bar{K}_1(x) \in G$. Therefore, it holds that

$$\mathbb{E} \left[\partial_{e_i} f_\gamma \left(x + \rho \frac{\nabla f_\gamma(x)}{\|\nabla f_\gamma(x)\|} \right) \right] \stackrel{(92)}{=} \partial_{e_i} f(x) + \rho \bar{K}_1(x) \quad (93)$$

Therefore, using assumption (89), $\forall i = 1, \dots, d$, we have that

$$\mathbb{E} \bar{\Delta}_i = -\partial_i f(x) \eta + \eta \rho \bar{K}_i(x) = \partial_{e_i} f(x) \eta + \mathcal{O}(\eta^2) \quad (94)$$

Additionally, by keeping in mind the definition of the covariance matrix Σ , We immediately have

$$\begin{aligned} \mathbb{E} \bar{\Delta}_i \bar{\Delta}_j &\stackrel{(92)}{=} \text{Cov}(\bar{\Delta}_i, \bar{\Delta}_j) + \mathbb{E} \bar{\Delta}_i \mathbb{E} \bar{\Delta}_j \\ &= \Sigma_{(ij)}^{SGD} \eta^2 + \partial_i f \partial_j f \eta^2 + \eta^2 \rho (\partial_i f \bar{K}_j(x) + \partial_j f \bar{K}_i(x)) + \eta^2 \rho^2 \bar{K}_i(x) \bar{K}_j(x) \\ &= \Sigma_{(ij)}^{SGD} \eta^2 + \partial_i f \partial_j f \eta^2 + \mathcal{O}(\eta^2 \rho) + \mathcal{O}(\eta^2 \rho^2) \\ &= \partial_i f \partial_j f \eta^2 + \Sigma_{(ij)}^{SGD} \eta^2 + \mathcal{O}(\eta^3) \quad \forall i, j = 1, \dots, d \end{aligned} \quad (95)$$

Finally, with analogous considerations, it is obvious that under our assumptions

$$\mathbb{E} \prod_{j=1}^s \bar{\Delta}_{i_j} = \mathcal{O}(\eta^3) \quad \forall s \geq 3, \quad i_j \in \{1, \dots, d\}.$$

□

Proof of Theorem 19. To prove this result, all we need to do is check the conditions in Theorem 10. As we apply Lemma 9, we make the following choices:

- $b(x) = -\nabla f(x)$,
- $\sigma(x) = \Sigma^{\text{SGD}}(X_t)^{\frac{1}{2}}$;

First of all, we notice that $\forall i = 1, \dots, d$, it holds that

- $\mathbb{E}\bar{\Delta}_i \stackrel{1. \text{ Lemma } 20}{=} -\partial_i f(x)\eta + \mathcal{O}(\eta^2)$;
- $\mathbb{E}\Delta_i \stackrel{1. \text{ Lemma } 9}{=} -\partial_i f(x)\eta + \mathcal{O}(\eta^2)$.

Therefore, we have that for some $K_1(x) \in G$

$$|\mathbb{E}\Delta_i - \mathbb{E}\bar{\Delta}_i| \leq K_1(x)\eta^2, \quad \forall i = 1, \dots, d. \quad (96)$$

Additionally, we notice that $\forall i, j = 1, \dots, d$, it holds that

- $\mathbb{E}\bar{\Delta}_i \bar{\Delta}_j \stackrel{2. \text{ Lemma } 20}{=} \partial_i f \partial_j f \eta^2 + \Sigma_{(ij)}^{\text{SGD}} \eta^2 + \mathcal{O}(\eta^3)$;
- $\mathbb{E}\Delta_i \Delta_j \stackrel{2. \text{ Lemma } 9}{=} \partial_i f \partial_j f \eta^2 + \Sigma_{(ij)}^{\text{SGD}} \eta^2 + \mathcal{O}(\eta^3)$.

Therefore, we have that for some $K_2(x) \in G$

$$|\mathbb{E}\Delta_i \Delta_j - \mathbb{E}\bar{\Delta}_i \bar{\Delta}_j| \leq K_2(x)\eta^2, \quad \forall i, j = 1, \dots, d \quad (97)$$

Additionally, we notice that $\forall s \geq 3, \forall i_j \in \{1 \dots d\}$, it holds that

- $\mathbb{E} \prod_{j=1}^s \bar{\Delta}_{i_j} \stackrel{3. \text{ Lemma } 20}{=} \mathcal{O}(\eta^3)$;
- $\mathbb{E} \prod_{j=1}^s \Delta_{i_j} \stackrel{3. \text{ Lemma } 9}{=} \mathcal{O}(\eta^3)$.

Therefore, we have that for some $K_3(x) \in G$

$$\left| \mathbb{E} \prod_{j=1}^s \Delta_{i_j} - \mathbb{E} \prod_{j=1}^s \bar{\Delta}_{i_j} \right| \leq K_3(x)\eta^2. \quad (98)$$

Additionally, for some $K_4(x) \in G, \forall i_j \in \{1 \dots d\}$

$$\mathbb{E} \prod_{j=1}^3 |\bar{\Delta}_{(i_j)}| \stackrel{3. \text{ Lemma } 20}{\leq} K_4(x)\eta^2. \quad (99)$$

Finally, Eq. (96), Eq. (97), Eq. (98), and Eq. (99) allow us to conclude the proof. \square

B Convergence Analysis: Quadratic Loss

B.1 ODE USAM

Let us study the quadratic loss function $f(x) = x^\top Hx$ where H is a diagonal matrix of eigenvalues $(\lambda_1, \dots, \lambda_d)$ such that $\lambda_1 \geq \lambda_2 \geq \dots \geq \lambda_d$. Under the dynamics of the ODE of USAM, we have that

$$dX_t = -H(X_t + \rho H X_t) = -H(I + \rho H)X_t, \quad (100)$$

which, for the single component gives us the following dynamics

$$dX_t^j = -\lambda_j(1 + \rho\lambda_j)X_t^j \quad (101)$$

whose solution is

$$X_t^j = X_0^j e^{-\lambda_j(1+\rho\lambda_j)t}. \quad (102)$$

Lemma 21. *For all $\rho > 0$, if all the eigenvalues of H are positive, then*

$$X_t^j \xrightarrow{t \rightarrow \infty} 0, \quad \forall j \in \{1, \dots, d\} \quad (103)$$

Proof of Lemma 21. For each $j \in \{1, \dots, d\}$, we have that

$$X_t^j = X_0^j e^{-\lambda_j(1+\rho\lambda_j)t}.$$

Therefore, since the exponent is always negative, $X_t^j \rightarrow 0$ as $t \rightarrow \infty$. □

Lemma 22. *Let H have at least one strictly negative eigenvalue and let λ_* be the largest negative eigenvalue of H . Then, for all $\rho > -\frac{1}{\lambda_*}$,*

$$X_t^j \xrightarrow{t \rightarrow \infty} 0, \quad \forall j \in \{1, \dots, d\}. \quad (104)$$

Proof of Lemma 22. For each $j \in \{1, \dots, d\}$, we have that

$$X_t^j = X_0^j e^{-\lambda_j(1+\rho\lambda_j)t}.$$

Therefore, if $\lambda_j > 0$, the exponent is always negative for each value of $\rho > 0$. Therefore, $X_t^j \rightarrow 0$ as $t \rightarrow \infty$. Differently, if $\lambda_j < 0$, the exponent $-\lambda_j(1+\rho\lambda_j)$ is negative only if $\rho > -\frac{1}{\lambda_*}$ where λ_* is the largest negative eigenvalue of H . Therefore, if $\rho > -\frac{1}{\lambda_*}$, $X_0^j \rightarrow 0$ if $t \rightarrow \infty$. □

B.2 SDE USAM - Stationary Distribution

Let us consider the noisy quadratic model $f(x) = \frac{1}{2}x^\top Hx$, where H is a symmetric matrix. Then, based on Theorem (11) and assuming $\Sigma(x) = \varsigma I$, the corresponding SDE is give by

$$dX_t = -H(I + \rho H)X_t dt + [(I + \rho H)\sqrt{\eta}\varsigma] dW_t. \quad (105)$$

Theorem 23 (Stationary distribution - PSD Case.). *For any $\rho > 0$, the stationary distribution of Eq. (105) is*

$$P(x, \infty | \rho) = \sqrt{\frac{2\lambda_i}{\pi\eta\varsigma^2}} \frac{1}{1 + \rho\lambda_i} \exp\left[-\frac{2\lambda_i}{\eta\varsigma^2} \frac{1}{1 + \rho\lambda_i} x^2\right] \quad (106)$$

where $(\lambda_1, \dots, \lambda_d)$ are the eigenvalues of H and $\lambda_i > 0, \forall i \in \{1, \dots, d\}$.

More interestingly, if ρ is too large, this same conclusion holds even for a saddle point.

Theorem 24 (Stationary distribution - Indefinite Case.). *Let $(\lambda_1, \dots, \lambda_d)$ are the eigenvalues of H such that there exists at least one which is strictly negative. If $\rho > -\frac{1}{\lambda_*}$ where λ_* is the largest negative eigenvalue of H , then the stationary distribution of Eq. (105) is*

$$P(x, \infty | \rho) = \sqrt{\frac{2\lambda_i}{\pi\eta\varsigma^2}} \frac{1}{1 + \rho\lambda_i} \exp\left[-\frac{2\lambda_i}{\eta\varsigma^2} \frac{1}{1 + \rho\lambda_i} x^2\right] \quad (107)$$

Proof of Theorem 23. Note that Eq. (105) is a linear SDE, and that drift and diffusion matrices are co-diagonalizable: Let $H = U\Lambda U^\top$ be one eigenvalue decomposition of H , with $\Lambda = \text{diag}(\lambda_1, \dots, \lambda_d)$. If we plug this in, we get

$$dX_t = -U(\Lambda + \rho\Lambda^2)U^\top X_t dt + U[(I + \rho\Lambda)\sqrt{\eta\varsigma}]U^\top dW_t.$$

Let us multiply the LHS with U^\top , then

$$d(U^\top X_t) = -(\Lambda + \rho\Lambda^2)(U^\top X_t)dt + [(I + \rho\Lambda)\sqrt{\eta\varsigma}]U^\top dW_t.$$

Finally, note that $U^\top dW_t = dW_t$ in law, so we can write

$$d(U^\top X_t) = -(\Lambda + \rho\Lambda^2)(U^\top X_t)dt + [(I + \rho\Lambda)\sqrt{\eta\varsigma}]dW_t.$$

This means that the coordinates of the vector $Y = U^\top X$ evolve independently

$$dY_t = -(\Lambda + \rho\Lambda^2)Y_t dt + [(I + \rho\Lambda)\sqrt{\eta\varsigma}]dW_t,$$

since Λ is diagonal. Therefore for the i -th component Y_i we can write

$$dY_{i,t} = -(\lambda_i + \rho\lambda_i^2)Y_{i,t}dt + [(1 + \rho\lambda_i)\sqrt{\eta\varsigma}]dW_{i,t}. \quad (108)$$

Note that this is a simple one-dimensional Ornstein–Uhlenbeck process $dY_t = -\theta Y_t dt + \sigma dW_t$ ($\theta > 0, \sigma \neq 0$) with parameters

$$\theta = \lambda_i(1 + \rho\lambda_i) > 0 \quad \text{and} \quad \sigma = (1 + \rho\lambda_i)\sqrt{\eta\varsigma} > 0 \quad (109)$$

Therefore, from Section 4.4.4 of (Gardiner et al., 1985), we get that

$$\mathbb{E}[Y_t] = e^{-\theta t}Y_0, \quad \text{Var}(Y_t) = \frac{\sigma^2}{2\theta}(1 - e^{-2\theta t}). \quad (110)$$

In our case we have that

$$\mathbb{E}[Y_t] = e^{-\theta t}Y_0 \rightarrow 0 \quad \text{and} \quad \text{Var}(Y_t) = \frac{\sigma^2}{2\theta}(1 - e^{-2\theta t}) \rightarrow \frac{\sigma^2}{2\theta} = \frac{\eta\varsigma^2}{2\lambda_i}(1 + \rho\lambda_i). \quad (111)$$

Additionally, using the Fokker–Planck equation, see Section 5.3 of (Risken, 1996), we have the following formula for the stationary distribution of each eigendirection. Indeed, let us recall that for $D := \frac{\sigma^2}{2}$, the probability density function is

$$P(x, t | x', t', \rho) = \sqrt{\frac{\theta}{2\pi D(1 - e^{-2\theta(t-t')})}} \exp\left[-\frac{\theta}{2D} \frac{(x - x'e^{-\theta(t-t')})^2}{1 - e^{-2\theta(t-t')}}\right]. \quad (112)$$

Therefore, the stationary distribution is

$$\begin{aligned} P(x, \infty | \rho) &= \sqrt{\frac{\theta}{2\pi D}} \exp\left[-\frac{\theta}{2D}x^2\right] \\ &= \sqrt{\frac{\theta}{\pi\sigma^2}} \exp\left[-\frac{\theta}{\sigma^2}x^2\right] \\ &= \sqrt{\frac{2\lambda_i}{\pi\eta\varsigma^2}} \frac{1}{1 + \rho\lambda_i} \exp\left[-\frac{2\lambda_i}{\eta\varsigma^2} \frac{1}{1 + \rho\lambda_i} x^2\right]. \end{aligned} \quad (113)$$

To conclude,

$$Y_{i,\infty} \sim \mathcal{N}\left(0, \frac{\eta\varsigma^2}{2\lambda_i}(1 + \rho\lambda_i)\right). \quad (114)$$

Since all of the eigenvalues are positive, this distribution has more variance than SGD on each direction. \square

Since the proof of Theorem 24 is perfectly similar to that of Theorem 23, we skip it. Additionally, a very analogous result holds true even if all the eigenvalues are strictly negative and thus the quadratic has a single maximum as a critical point. From these results, we understand that under certain circumstances, USAM might be attracted not only by the minimum but possibly also by a saddle or a maximum. This is fully consistent with the results derived for the ODE of USAM in Lemma 21 and Lemma 22.

Observation 25 (Suboptimality under the Stationary Distribution – comparison to SGD). *In the special case where the stochastic process has reached stationarity, one can approximate the loss landscape with a quadratic loss (Jastrzebski et al., 2017). By further assuming that $\Sigma^{SGD}(x) = H$ (see e.g. Sagun et al. (2017); Zhu et al. (2018)), Theorem (11) implies that for USAM*

$$dX_t = -H(I + \rho H)X_t dt + \left[(I + \rho H)\sqrt{\eta}\sqrt{H}\right]dW_t. \quad (115)$$

Up to a change of variable, we assume H to be diagonal and therefore

$$\mathbb{E}_{USAM}[f] = \frac{1}{2} \sum_{i=1}^d \lambda_i \mathbb{E}[X_i^2] = \frac{\eta}{4} \sum_{i=1}^d \lambda_i (1 + \rho\lambda_i)^2 = \frac{\eta}{4} (Tr(H) + 2\rho Tr(H^2) + \rho^2 Tr(H^3)) \gg \mathbb{E}_{SGD}[f], \quad (116)$$

where subscripts indicate that f is being optimized with SGD and USAM, respectively.

Regarding SAM, Theorem (16) implies that

$$dX_t = -H \left(I + \frac{\rho H}{\|HX_t\|} \right) X_t + \sqrt{\eta}\sqrt{H} \left(I + \frac{\rho H}{\|HX_t\|} \right) dW_t. \quad (117)$$

Therefore, we argue that SAM has to have a suboptimality with respect to SGD which is even larger than that of USAM. Intuitively, when $\|HX_t\| < 1$, the variance of SAM is larger than that of USAM. Therefore, its suboptimality has to be larger as well.

B.3 ODE SAM

W.l.o.g, we take H to be diagonal and if it has negative eigenvalues, we denote the largest negative eigenvalue with λ_* . Let us recall that the ODE of SAM for the quadratic loss is given by

$$dX_t = -H \left(I + \frac{\rho H}{\|HX_t\|} \right) X_t \quad (118)$$

Lemma 26. *For all $\rho > 0$, if H is PSD, the origin is (locally) asymptotically stable. Additionally, if H is not PSD, if $\|HX_t\| \leq -\rho\lambda_*$, then the origin is still (locally) asymptotically stable.*

Proof of Lemma 26. Let $V(x) := \frac{x^\top K x}{2}$ be the Lyapunov function, where K is a diagonal matrix with positive eigenvalues (k_1, \dots, k_d) . Therefore, we have

$$V(X_t) = \frac{1}{2} \sum_{i=1}^d k_i (X_t^i)^2 > 0 \quad (119)$$

and

$$\dot{V}(X_t) = \sum_{i=1}^d k_i X_t^i \dot{X}_t^i = \sum_{i=1}^d k_i (-\lambda_i) \left(1 + \frac{\rho \lambda_i}{\|HX_t\|} \right) X_t^i X_t^i = - \sum_{i=1}^d k_i \lambda_i \left(1 + \frac{\rho \lambda_i}{\|HX_t\|} \right) (X_t^i)^2. \quad (120)$$

Let us analyze the terms

$$k_i \lambda_i \left(1 + \frac{\rho \lambda_i}{\|HX_t\|} \right) (X_t^i)^2.$$

When $\lambda_i > 0$, these quantities are all positive and the proof is concluded. However, if there exists $\lambda_i < 0$, these quantities are positive only if $\left(1 + \frac{\rho \lambda_i}{\|HX_t\|} \right) \leq 0$, that is if $\|HX_t\| \leq -\rho \lambda_i$. Therefore, a sufficient condition for $\dot{V}(X_t) \leq 0$ is that

$$\|HX_t\| \leq -\rho \lambda_i, \quad \forall i \text{ s.t. } \lambda_i < 0.$$

Based on Theorem 1.1 of Mao (2007), we conclude that if $\|HX_t\| \leq -\rho$ where λ_* is the largest negative eigenvalue of H , $V(X_t) > 0$ and $\dot{V}(X_t) \leq 0$, and that therefore the dynamics of X_t is bounded inside this compact set and cannot diverge. \square

From this result, we understand that the dynamics of the ODE of USAM might converge to a saddle or even a maximum if it gets too close to it.

B.4 SDE SAM

W.l.o.g, we take H to be diagonal and if it has negative eigenvalues, we denote the largest negative eigenvalue with λ_* . Based on Eq. (20) and assuming $\Sigma^{\text{SGD}} = \varsigma^2 I$, SDE of SAM for the quadratic loss is given by

$$dX_t = -H \left(I + \frac{\rho H}{\|HX_t\|} \right) X_t + \sqrt{\eta} \varsigma \left(I + \frac{\rho H}{\|HX_t\|} \right) dW_t \quad (121)$$

Observation 27. *For all $\rho > 0$, there exists an $\epsilon > 0$ such that if $\|HX_t\| \in (\epsilon, -\rho\lambda_*)$, the dynamics of X_t is attracted towards the origin. If the eigenvalues are all positive, the condition is $\|HX_t\| \in (\epsilon, \infty)$. On the contrary, if $\|HX_t\| < \epsilon$, then the dynamics is pushed away from the origin.*

Formal calculations to support Observation 27. Let $V(t, x) := e^{-t \frac{x^\top K x}{2}}$ be the Lyapunov function, where K is a diagonal matrix with strictly positive eigenvalues (h_1, \dots, h_d) . Therefore, we have

$$V(X_t) = e^{-t} \frac{1}{2} \sum_{i=1}^d k_i (X_t^i)^2 > 0 \quad (122)$$

and

$$\begin{aligned} LV(t, X_t) &= -e^{-t} \frac{1}{2} \sum_{i=1}^d k_i (X_t^i)^2 + e^{-t} \sum_{i=1}^d k_i (-\lambda_i) \left(1 + \frac{\rho \lambda_i}{\|HX_t\|} \right) (X_t^i)^2 + e^{-t} \frac{\eta \varsigma^2}{2} \sum_{i=1}^d k_i \left(1 + \frac{\rho \lambda_i}{\|HX_t\|} \right)^2 \\ &= -e^{-t} \left(\frac{1}{2} \sum_{i=1}^d k_i (X_t^i)^2 + \sum_{i=1}^d k_i \lambda_i \left(1 + \frac{\rho \lambda_i}{\|HX_t\|} \right) (X_t^i)^2 - \frac{\eta \varsigma^2}{2} \sum_{i=1}^d k_i \left(1 + \frac{\rho \lambda_i}{\|HX_t\|} \right)^2 \right) \end{aligned} \quad (123)$$

Let us analyze the terms

$$k_i \lambda_i \left(1 + \frac{\rho \lambda_i}{\|HX_t\|} \right) (X_t^i)^2.$$

When $\lambda_i > 0$, these quantities are all positive. When $\lambda_i < 0$, these quantities are positive only if $\left(1 + \frac{\rho \lambda_i}{\|HX_t\|} \right) \leq 0$, that is if $\|HX_t\| \leq -\rho \lambda_i$. Let us now assume that

$$\|HX_t\| \leq -\rho \lambda_i, \quad \forall i \text{ s.t. } \lambda_i < 0.$$

that is, $\|HX_t\| \leq -\rho \lambda_*$ such that λ_* . Then, we observe that

- If $\|HX_t\| \rightarrow 0$, $LV(t, X_t) \geq 0$
- If ς is small enough, for $\|HX_t\| \approx -\rho \lambda_*$, $LV(t, X_t) \leq 0$

Given that all functions and functionals involved are continuous, there exists $\epsilon > 0$ such that

- If $\|HX_t\| < \epsilon$, $LV(t, X_t) \geq 0$
- If ς is small enough, for $\|HX_t\| \in (\epsilon, -\rho \lambda_*)$, $LV(t, X_t) \leq 0$

□

Based on Theorem 2.2 of Mao (2007), we understand that if the dynamics is sufficiently close to the origin, it gets pulled towards it, but if gets too close, it gets repulsed from it. If there is no negative eigenvalue, the same happens but the dynamics can never get close to the minimum.

C Experiments

In this Section, we provide additional details regarding the validation that the SDEs we proposed indeed weakly approximate the respective algorithms. We do so on a quadratic landscape and on a binary classification task for both a shallow and a deep linear model. Since our SDEs prescribe the calculation of the Hessian of the whole neural network at each iteration step, this precludes us from testing our theory on large-scale models.

C.1 SDE Validation

Quadratic In this paragraph, we provide the details of the Quadratic experiment. We optimize the loss function $f(x) = \frac{1}{2}x^\top Hx$ of dimension $d = 20$. The Hessian H is a random SPD matrix generated using the standard Gaussian matrix $A \in \mathbb{R}^{d \times 2d}$ as $H = AA^\top/(2d)$. The noise used to perturb the gradients is $Z \sim \mathcal{N}(0, \Sigma)$ where $\Sigma = \sigma I_d$ and $\sigma = 0.01$. We use $\eta = 0.01$, $\rho \in \{0.001, 0.01, 0.1, 0.5\}$. The results are averaged over 3 experiments.

Shallow Linear Classification In this paragraph, we provide the details for the Shallow Linear Classification experiment. This is a binary classification task and we optimize the loss function $f(x) = \frac{1}{n} \sum_{i=1}^n \log(1 + \exp(y_i \cdot a_i^\top x)) + \frac{\lambda}{2} \|x\|^2$ where $a_i \in \mathbb{R}^d$ is the feature vector for the i -th datapoint, $y_i \in \{-1, 1\}$ is the corresponding binary target and $\lambda = 0.1$. The parameter optimized is $x \in \mathbb{R}^d$. We use the Breast Cancer Database Dua and Graff (2017), therefore the dimension of the datapoints is $d = 39$ and the number of datapoints is $n = 569$. The noise used to perturb the gradients is $Z \sim \mathcal{N}(0, \Sigma)$ where $\Sigma = \sigma I_d$ and $\sigma = 0.01$. We use $\eta = 0.01$, $\rho \in \{0.001, 0.01, 0.1, 0.5\}$. The results are averaged over 3 experiments.

Deep Linear Classification In this paragraph, we provide the details for the Shallow Linear Classification experiment. This is a binary classification task and we optimize the loss function $f(x) = \frac{1}{n} \sum_{i=1}^n \log(1 + \exp(y_i \cdot a_i^\top x_1 x_2)) + \frac{\lambda}{2} \|x\|^2$ where $a_i \in \mathbb{R}^d$ is the feature vector for the i -th datapoint, $y_i \in \{-1, 1\}$ is the corresponding binary target and $\lambda = 0.1$. The parameter optimized is $x = [x_1, x_2]$ where $x_1 \in \mathbb{R}^{d \times d}$ and $x_2 \in \mathbb{R}^{d \times 1}$. We use the Breast Cancer Database Dua and Graff (2017), therefore the dimension of the datapoints is $d = 39$ and the number of datapoints is $n = 569$. The noise used to perturb the gradients is $Z \sim \mathcal{N}(0, \Sigma)$ where $\Sigma = \sigma I_d$ and $\sigma = 0.01$. We use $\eta = 0.01$, $\rho \in \{0.001, 0.01, 0.1, 0.5\}$. The results are averaged over 3 experiments.

C.2 Quadratic Landscape

Interplay Between Hessian, ρ , and the noise. In this paragraph, we provide additional details regarding the interplay between the Hessian, ρ , and the noise. In the first experiment represented in Figure 5, we fix $\rho = \sqrt{\eta}$, where $\eta = 0.001$ is the learning rate. Then, we fix the Hessian $H \in \mathbb{R}^{100 \times 100}$ to be diagonal with random positive eigenvalues. Then, we select the scaling factors $\sigma \in \{1, 2, 4\}$. For each value of σ , we optimize the quadratic loss with SGD and SAM where the hessian is scaled up by a factor σ . The starting point is $x_0 = (0.02, \dots, 0.02)$ and the number of iterations is 20000. The results are averaged over 100 runs.

In the second experiment represented in Figure 7, we fix the Hessian H with random positive eigenvalues. then, we select $\rho = \sqrt{\eta}$, where $\eta = 0.001$ is the learning rate. Then, we select the scaling factors $\sigma \in \{1, 2, 4\}$. For each value of σ , we optimize the quadratic loss with SGD and SAM where the hessian is fixed and ρ is scaled up by a factor σ . The starting point is $x_0 = (0.02, \dots, 0.02)$ and the number of iterations is 20000. The results are averaged over 100 runs.

The very same setup holds for the experiments carried out for USAM and represented in Figure 6 and Figure 8.

Stationary Distribution Convex Case In this paragraph, we provide the details of the experiment about the dynamics of the SDE of SAM in the quadratic convex case of dimension 2. The hessian is diagonal with both eigenvalues equal to 1. We select $\rho = \sqrt{\eta}$, where $\eta = 0.001$ is the learning rate. In the first image on the left of Figure 9, we show the distribution of 10^5 trajectories all starting at $(0.02, 0.02)$ after $5 \cdot 10^4$ iterations. In the second image, we plot the number of trajectories that at a certain time are inside a ball of radius 0.007, e.g. close to the origin. As we can see in greater detail in the third image, all of them are initialized outside such a ball, then they get attracted inside, and around the 600-th iteration they get repulsed out of it. We highlight that the proportion of points inside/outside the ball is relatively

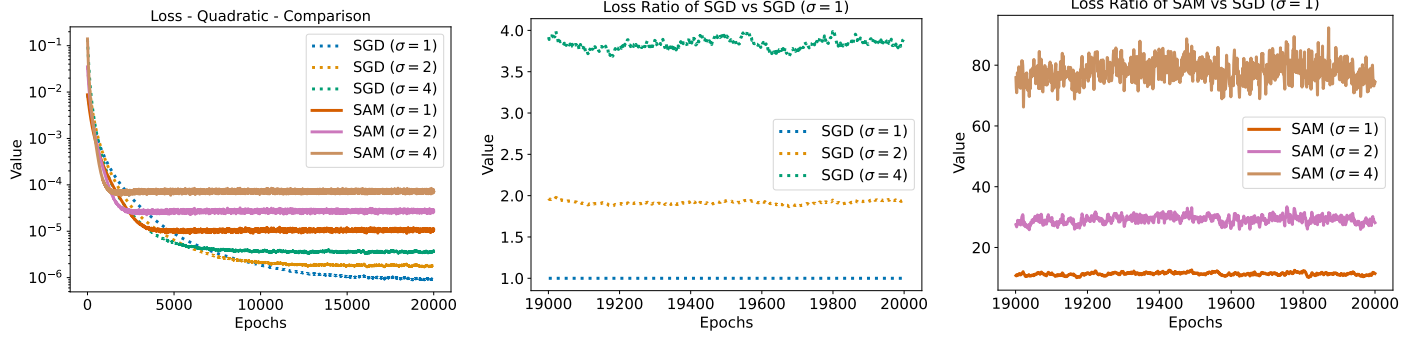


Figure 5: Role of the Hessian - Left: Comparison between SGD and SAM for fixed rho and larger Hessians. Center: Ratio between the Loss of SGD for different scaling of the Hessian by the loss of the unscaled case of SGD. Right: Ratio between the Loss of SAM for different scaling of the Hessian by the loss of the unscaled case of SGD.

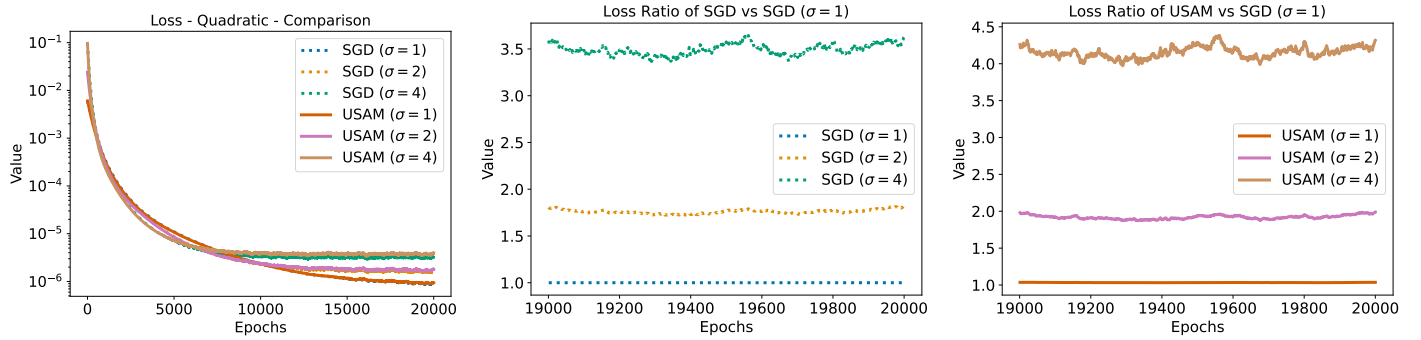


Figure 6: Role of the Hessian - Left: Comparison between SGD and USAM for fixed rho and larger Hessians. Center: Ratio between the Loss of SGD for different scaling of the Hessian by the loss of the unscaled case of SGD. Right: Ratio between the Loss of USAM for different scaling of the Hessian by the loss of the unscaled case of SGD.

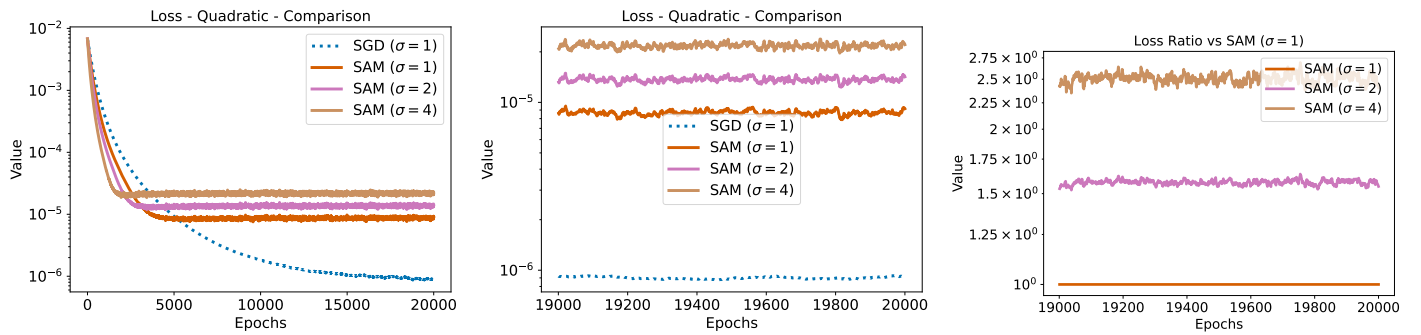


Figure 7: Role of ρ - Left: Comparison between SGD and SAM for fixed hessian and larger ρ values. Center: Zoom at convergence. Right: Ratio between the Loss of SAM for different scaling of the Hessian by the loss of the unscaled case of SAM.

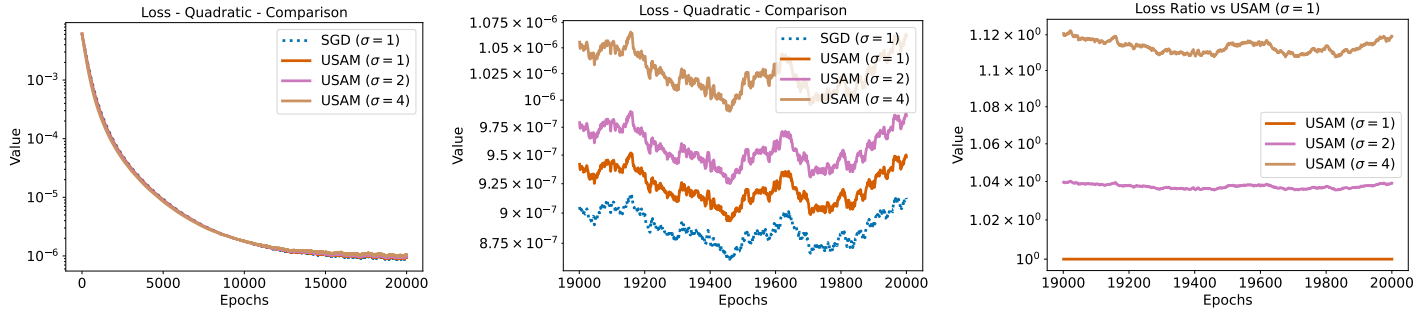


Figure 8: Role of ρ - Left: Comparison between SGD and USAM for fixed hessian and larger ρ values. Center: Zoom at convergence. Right: Ratio between the Loss of USAM for different scaling of the Hessian by the loss of the unscaled case of USAM.

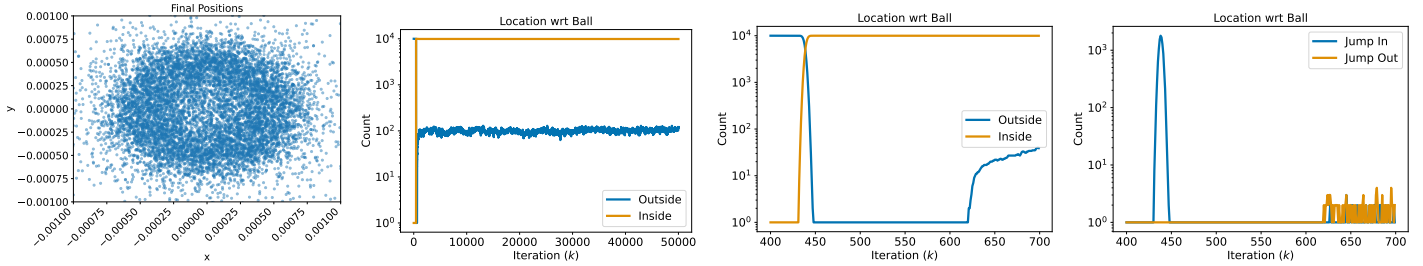


Figure 9: Convex Quadratic - Left: Distribution points around the origin is scarcer near to the origin; Center-Left: Number of trajectories outside a small ball around the origin increases over time; Center-Right: All the trajectories eventually enter the ball and then start exiting it; Right: There is a constant oscillation of points in and out of the ball.

stable. In the fourth image, we count the number of trajectories that are jumping in or out of such a ball. All of the trajectories enter the ball between the 400-th and 500-th iteration, and then they start jumping in and out after the iteration 600. We conclude that this experimental evidence are supporting the claim that the origin attracts the dynamics, but repulses it at the moment that the trajectories get too close to it.

Stationary Distribution Saddle Case In this paragraph, we provide the details of the experiment about the dynamics of the SDE of SAM in the quadratic saddle case of dimension 2. The hessian is diagonal with eigenvalues equal to 1 and -1 . We select $\rho = \sqrt{\eta}$, where $\eta = 0.001$ is the learning rate. In the first image on the left of Figure 3, we show the distribution of 10^5 trajectories all starting at $(0.02, 0.02)$ after $5 \cdot 10^4$ iterations. In the second image, we plot the number of trajectories that at a certain time are inside a ball of radius 0.007, e.g. close to the origin. As we can see in greater detail in the third image, all of them are initialized outside such a ball, then they get attracted inside, and around the 1200-th iteration they get repulsed out of it. We highlight that the proportion of points outside the ball is stably increasing, meaning that the trajectories are slowly escaping from the saddle. In the fourth image, we count the number of trajectories that are jumping in or out of such a ball. All of the trajectories enter the ball between the 950-th and 1000-th iteration, and then they start jumping in and out after the iteration 1200. We conclude that this experimental evidence are supporting the claim that the origin attracts the dynamics, but repulses it at the moment that the trajectories get too close to it, even when this is a saddle.

Escaping the Saddle - Low Dimensional In this paragraph, we provide details for the Escaping the Saddle experiment in dimension $d = 2$. As in the previous experiment, the saddle is a quadratic of

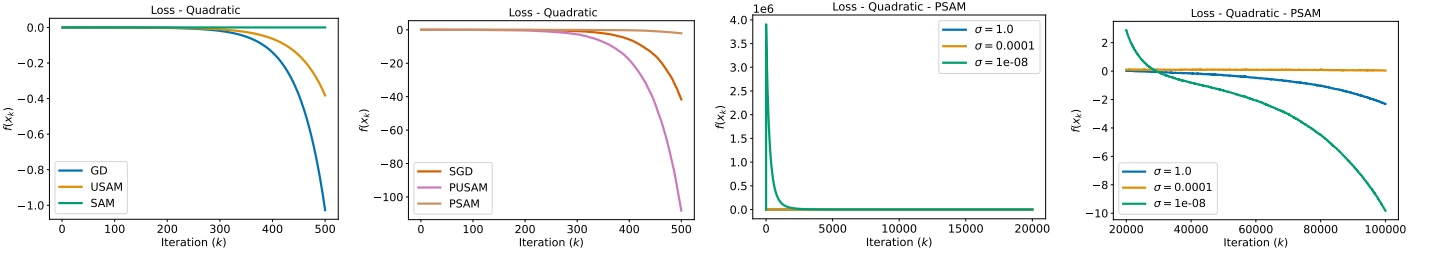


Figure 10: Escaping the Saddle - Left: Comparison between GD, SAM, and USAM at escaping from a quadratic saddle. Center-Left: Comparison between PGD, PSAM, and PUSAM at escaping from a quadratic saddle. Center-Right: PSAM escapes from the origin immediately due to a volatility spike. Right: The PSAM initialized far from the origin starts escaping from it; The PSAM which jumped away from it efficiently escapes the saddle.

dimension 2 and its hessian is diagonal with eigenvalues equal to 1 and -1 . We select $\rho = \sqrt{\eta}$, where $\eta = 0.001$ is the learning rate. We initialize the GD, USAM, SAM, SGD, PUSAM, and PSAM in the point $x_0 = (0, 0.01)$, e.g. in the direction of the fastest escape from the saddle. In the left of Figure 10, we observe that GD and USAM manage to escape the saddle while SAM remains stuck. We highlight that running for more iterations would not change this as SAM is oscillating across the origin. In the second figure, we observe that the stochastic optimizers escape the saddle quicker than their deterministic counterpart and even PSAM manages to escape. Results are averaged over 3 runs.

Escaping the Saddle - High Dimensional In this paragraph, we provide details for the Escaping the Saddle experiment in dimension $d = 400$. We fix the Hessian $H \in \mathbb{R}^{400 \times 400}$ to be diagonal with random positive eigenvalues. To simulate a saddle, we flip the sign of the smallest 10 eigenvalues. We select $\rho = \sqrt{\eta}$, where $\eta = 0.001$ is the learning rate. We study the optimization dynamics of PSAM as we initialize the process closer and closer to the saddle in the origin. The starting point $x_0 = (1, \dots, 1)$ is scaled with factors $\sigma \in \{10^0, 10^{-4}, 10^{-8}\}$ and we notice that the one scaled with $\sigma = 1$ escapes slowly from the saddle. The one scaled with $\sigma = 10^{-8}$ experiences a sharp spike in volatility and jumps away from the origin and ends up escaping the saddle faster than the previous case. Finally, the one scaled with $\sigma = 10^{-4}$ stays trapped in the saddle. Results are averaged over 3 runs.

C.3 Linear Autoencoder

In this paragraph, we provide additional details regarding the Linear Autoencoder experiment. In this experiment, we approximate the Identity matrix of dimension 20 as the product of two square matrices $W1$ and $W2$. As described in Kunin et al. (2019), there is a saddle of the loss function around the origin. Inspired by the results obtained for the quadratic landscape, we test if SAM and its variants struggle to escape this saddle as well. To do this, we initialize the two matrices with entries normally distributed. We select $\rho = \sqrt{\eta}$, where $\eta = 0.001$ is the learning rate. Then, we study the dynamics of the optimization process in case we scale the matrices by a factor σ equal to $10^{-2}, 10^{-3}, 5 \cdot 10^{-3}, 10^{-4}$, and 10^{-5} . As we can see from the first image of Figure 4, initializing SAM far from the origin, that is $\sigma = 0.01$, allows SAM to optimize the loss. Decreasing σ implies that SAM becomes slower and slower at escaping the loss up to not being able to escape it anymore. The second image shows that the very same happens if we use PSAM. However, if the process is initialized extremely close to the origin, that is $\sigma = 10^{-5}$, then the process enjoys a volatility spike that pushes it away from the origin. This allows the process to escape the saddle quickly and effectively. In the fourth image, we compare the behavior of GD, USAM, SAM, PGD, PUSAM, and PSAM where $\sigma = 10^{-5}$. We observe that PSAM is the fastest algorithm to escape the saddle, followed by GD, SGD, PUSAM, USAM, and finally, SAM does not escape. Results are averaged over 3 runs.

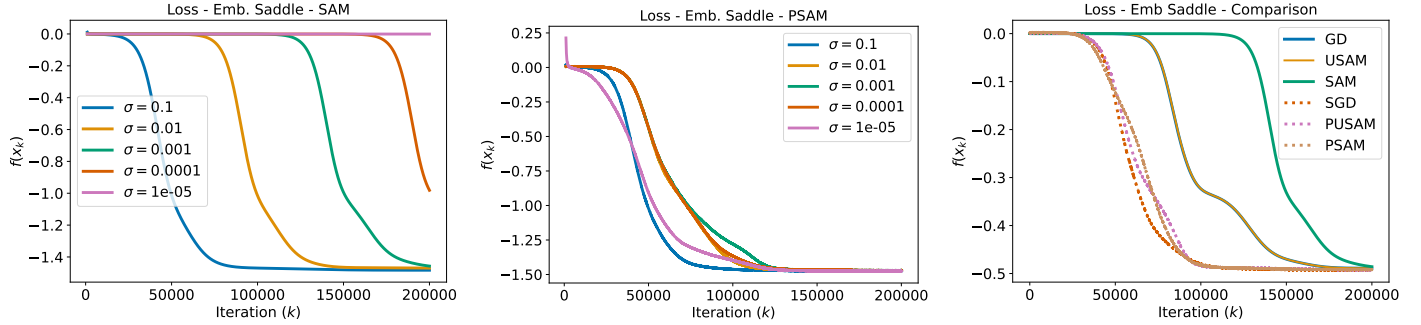


Figure 11: Embedded Saddle - Left: SAM does not escape the saddle if it is too close to it. Center: PSAM always escapes it, but more slowly if initialized closer to the origin. If extremely close, it recovers speed thanks to a volatility spike. Right: SAM is stuck.

C.4 Embedded Saddle

In this paragraph, we provide additional details regarding the Embedded Saddle experiment. In this experiment, we optimize a regularized quadratic d -dimensional landscape $L(x) = \frac{1}{2}x^\top Hx + \lambda \sum_{i=1}^d x_i^4$. As described in Lucchi et al. (2022), if H is not PSD, there is a saddle of the loss function around the origin and local minima away from it. We fix the Hessian $H \in \mathbb{R}^{400 \times 400}$ to be diagonal with random positive eigenvalues. To simulate a saddle, we flip the sign of the smallest 10 eigenvalues. The regularization parameter is fixed at $\lambda = 0.001$. We use $\eta = 0.005$, $\rho = \sqrt{\eta}$, run for 200000 and average over 3 runs.

In Figure 11 we see the very same observations we had for the Autoencoder.